Transfer of Complexed and Dissociated Ionic Species at Soft Interfaces: Voltammetric Study of Chemical Kinetic and Diffusional Effects

Eduardo Laborda, José Manuel Olmos, Ángela Molina*

Departamento de Química Física, Facultad de Química, Regional Campus of International Excellence "Campus Mare Nostrum", Universidad de Murcia, 30100 Murcia, Spain

* Corresponding author:

Tel: +34 868 88 7524

Fax: +34 868 88 4148

Email: amolina@um.es

Abstract

A new transfer mechanism is considered in which two different ionic species of the same charge can be transferred across a soft interface while they interconvert with each other in the original phase through a homogeneous chemical reaction: the aqueous complexation-dissociation coupled to transfer (ACDT) mechanism. This can correspond to a free ion in aqueous solution in the presence of a neutral ligand that complexes it leading to a species that can be more or less lipophilic than the free ion. As a result, the transfer to the organic phase can be facilitated or hindered by the aqueous-phase chemical reaction.

Rigorous and approximate explicit analytical solutions are derived for the study of the above mechanism via normal pulse voltammetry, derivative voltammetry and chronoamperometry at macrointerfaces. The solutions enable us to examine the process whatever the species' lipophilicity and diffusivity in each medium and the kinetics and thermodynamics of the chemical reaction in solution. Moreover, when the chemical reaction is at equilibrium, explicit expressions for cyclic voltammetry and square wave voltammetry are obtained. With this set of equations, the influence of the different physicochemical phenomena on the voltammetric response is studied as well as the most suitable strategies to characterization them.

Keywords: Ion transfer; Liquid|liquid interface; Chemical reactivity; Mass transport; Voltammetry

1. INTRODUCTION

The study of ion transfer processes across the interface between two immiscible electrolyte solutions (ITIES) has great interest and impact in many fields, such as liquid/liquid electrochemistry and liquid/liquid extraction, with important implications in the development of electrochemical sensors and the design of drugs [1, 2]. In addition, the interface between the two phases (usually an aqueous and an organic solutions) can be used as a simple model for ion transport at biological membranes, constituting a biomimetic medium suitable for studying processes fundamental in bio-catalysis or cellular respiration [3]. Thus, one of the parameters that can be extracted by electrochemical techniques is the standard Gibbs energy of the ion transfer, which is directly related to the ion's lipophilicity [1]. The diffusivity of the ion in each phase as well as its concentration can also be extracted in a fast, inexpensive and simple way [4-11]. These properties determine the distribution of the ionic species in biological systems and their potential application as a drug or drug carrier.

According to the above, the electrochemical methods are very powerful in the study of the transfer of ionic species across soft interfaces. Given the dynamic nature of real systems and of voltammetric techniques, the rigorous modelling of such processes requires taking into account the influence of the species' chemical reactivity and diffusivity in each phase. Thus, the heterogenous processes of ion transfer can be coupled with homogeneous chemical reactions (as occurred with the analogous electron transfer processes [12-14]), such as in the so-called facilitated or assisted ion transfer mechanisms. For example, in the TOC mechanism the ion transfer is promoted by a ligand present in the organic solution; *i.e.* there is a chemical reaction following the charge transfer that stabilizes the ion [15] (equivalent to the EC mechanism in electron transfer processes). Other possible transfer routes are the ACT mechanism (a chemical

reaction preceding the ion transfer, equivalent to the so-called CE mechanism) and the TIC mechanism (ion transfer by an interfacial chemical reaction) [16].

Electrochemical techniques can also be employed to characterize the thermodynamics (equilibrium constant) and the kinetics (rate constants) of the chemical reaction(s) (except for the TIC mechanism, where the current response is only a function of thermodynamic parameters [17]) and to elucidate the reaction mechanism [18-21]. In previous works, we have reported analytical expressions for the voltammetric response of the TOC and TIC mechanisms at macrointerfaces, as well as for the case of any number of chemical reactions at equilibrium preceding and following the ion transfer [22-25]. These theoretical developments have been employed to characterize the transfer of several protonated amines facilitated by the ionophore dibenzo-18-crown-6 from water to a solvent polymeric membrane [11, 26].

In this work, a new transfer mechanism is considered in which two different ionic species taking part in a chemical reaction with a neutral species can be transferred: the aqueous complexation-dissociation coupled to transfer (ACDT) mechanism (see Scheme I). This can correspond, for example, to the transfer of a free metal and its complex, provided that the ligand is neutral. From this mechanism two general scenarios can be envisaged: the situation where the complex is more lipophilic (and so the complexation “facilitates” the ion transfer) and that where the complex is less lipophilic (and then complexation “hinders” the transfer). In the limit when only one of the species can be transferred within the electrochemical window, the above two situations would correspond to the so-called ACT mechanism (aqueous complexation followed by transfer [18]) and to the ADT mechanism (aqueous dissociation followed by transfer [27]). Therefore, the theory reported here (which can also be applied to the study of equivalent electron transfer reaction schemes) can assist in getting further

physicochemical insight into ion transfer mechanisms in real systems, with potential impact in speciation studies, such as the determination of the availability of metals complexes and their corresponding beneficial or toxic properties [28-31]. Many experimental and modelling approaches to speciation and bioavailability/toxicity are based on equilibrium principles [27]. In contrast, the consideration of mass transport and chemical kinetic effects in the present theory for the ACDT mechanism enables us to analyze the dynamic aspects of speciation in a general and rigorous way. This is particularly interesting given that natural aquatic systems are generally subject to changing conditions and are practically never at chemical equilibrium [27, 32-35].

Rigorous and approximate explicit analytical equations for the chronoamperometric, normal pulse voltammetry (NPV) and derivative voltammetry (dNPV) responses of the ACDT mechanism are deduced under non-equilibrium conditions. A general expression is also reported for any voltammetric technique (such as cyclic voltammetry and square wave voltammetry) under total equilibrium conditions. In all cases, the influence of the difference between the formal transfer potentials of the ion and the complex on the shape and position of the voltammograms are analyzed. Moreover, different criteria are proposed for qualitative and quantitative kinetic and thermodynamic studies based on the variation of the electrochemical response with time and with the ligand concentration.

2. THEORY

2.1 Influence of the chemical kinetics: application of a constant potential

Let us consider the reversible transfer of cationic species from an aqueous solution (w) to an organic phase (o) in the form of two chemical species M^{z+} and ML^{z+} (ACDT mechanism)

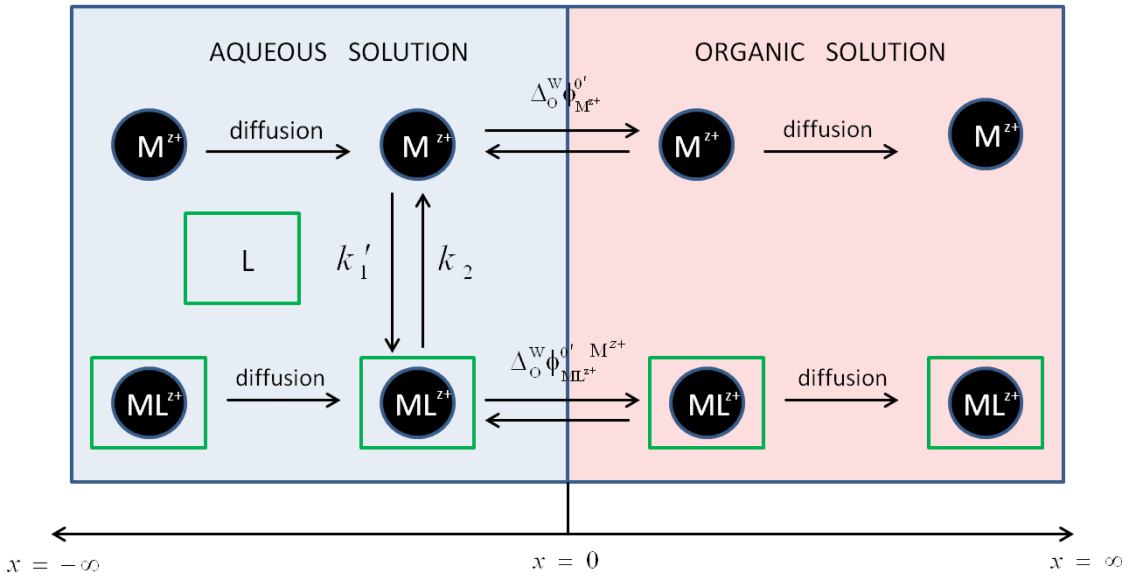

Scheme I

The above scheme can correspond to a free metal ion M^{z+} and its complex ML^{z+} in solution. In Scheme I, k_1' (M^{-1} s^{-1}) and k_2 (s^{-1}) are the forward and backward rate constants of the chemical reaction and $\Delta_O^W\phi^{0'}_{M^{z+}}$ and $\Delta_O^W\phi^{0'}_{ML^{z+}}$ are the formal ion transfer potentials of species M^{z+} and ML^{z+}, respectively. Moreover, the ligand L is assumed to be a neutral species present in a large excess in the aqueous solution, such that the kinetics of the chemical reaction can be considered of (pseudo)first order ($k_1 = k_1' c_L^*$ (s^{-1})). Under these conditions, the *conditional* or *apparent* equilibrium constant of complexation can be defined as follows

$$K = \frac{c_{ML}^*}{c_M^*} = \frac{k_1' c_L^*}{k_2} = K_c c_L^* \qquad (1)$$

with c_i^* (M) being the initial equilibrium concentration of species i ($i = M, ML, L$) in water and K_c (M^{-1}) the equilibrium constant based on concentrations.

When a constant potential difference E is applied between both phases with a length τ, supposing that diffusion is the only effective mass transport mechanism, the variations of the concentrations of the different species with the distance to the interface x and with the electrolysis time t ($0 \le t \le \tau$) are described by the following differential equation system

$$\left.\begin{aligned}
&\frac{\partial c_M^w(x,t)}{\partial t} = D_M^w \frac{\partial^2 c_M^w(x,t)}{\partial x^2} - k_1 c_M^w(x,t) + k_2 c_{ML}^w(x,t) \\
&\frac{\partial c_{ML}^w(x,t)}{\partial t} = D_{ML}^w \frac{\partial^2 c_{ML}^w(x,t)}{\partial x^2} + k_1 c_M^w(x,t) - k_2 c_{ML}^w(x,t) \\
&\frac{\partial c_M^o(x,t)}{\partial t} = D_M^o \frac{\partial^2 c_M^o(x,t)}{\partial x^2} \\
&\frac{\partial c_{ML}^o(x,t)}{\partial t} = D_{ML}^o \frac{\partial^2 c_{ML}^o(x,t)}{\partial x^2}
\end{aligned}\right\} \qquad (2)$$

where D_i^α is the diffusion coefficient of species i in phase α ($\alpha = w, o$). The boundary conditions associated to the system (2) are given by

$$\left.\begin{aligned} &x \le 0, t = 0 \\ &x \to -\infty, t \ge 0 \end{aligned}\right\} \qquad c_M^w = c_M^* \;\; ; \;\; c_{ML}^w = c_{ML}^* \qquad (3)$$

$$\left.\begin{aligned} &x \ge 0, t = 0 \\ &x \to \infty, t \ge 0 \end{aligned}\right\} \qquad c_M^o = c_{ML}^o = 0 \qquad (4)$$

$$x = 0, t > 0\}$$

$$D_M^w \left(\frac{\partial c_M^w}{\partial x}\right)_{x=0} = D_M^o \left(\frac{\partial c_M^o}{\partial x}\right)_{x=0} \qquad (5)$$

$$D_{ML}^w \left(\frac{\partial c_{ML}^w}{\partial x}\right)_{x=0} = D_{ML}^o \left(\frac{\partial c_{ML}^o}{\partial x}\right)_{x=0} \qquad (6)$$

$$c_M^o(0) = c_M^w(0) e^{\eta_1} \qquad (7)$$

$$c_{ML}^{o}(0) = c_{ML}^{w}(0)\mathrm{e}^{\eta_2} \tag{8}$$

with

$$\eta_1 = \frac{zF}{RT}\left(E - \Delta_{\mathrm{O}}^{\mathrm{W}}\phi_{\mathrm{M}^{z+}}^{0'}\right) \tag{9}$$

$$\eta_2 = \frac{zF}{RT}\left(E - \Delta_{\mathrm{O}}^{\mathrm{W}}\phi_{\mathrm{ML}^{+}}^{0'}\right) \tag{10}$$

where *F*, *R* and *T* have their usual meanings. Moreover, the current measured can be calculated by means of the following expression

$$I = -zFA\left[D_M^w\left(\frac{\partial c_M^w}{\partial x}\right)_{x=0} + D_{ML}^w\left(\frac{\partial c_{ML}^w}{\partial x}\right)_{x=0}\right] \tag{11}$$

where *A* is the interfacial area.

Now, we assume that the diffusion coefficients in a given phase are equal ($D_M^w = D_{ML}^w = D_w$ and $D_M^o = D_{ML}^o = D_o$) but different for the aqueous and organic solutions ($D_w \neq D_o$). Indeed, important differences are frequently observed in the diffusivity of ionic species in transfer processes between two immiscible electrolyte solutions, such as water and RTILs or solvent polymeric membranes [11, 36-38]. By defining two new variables [14]

$$\xi = c_M^w + c_{ML}^w \tag{12}$$

$$\phi = \left(Kc_M^w - c_{ML}^w\right)e^{(k_1+k_2)t} \tag{13}$$

with ϕ referring to the perturbation of the chemical equilibrium and ξ to the total concentration in the aqueous solution, Eqs. (2)-(8) are transformed as follows

$$\left.\begin{aligned}
\frac{\partial \xi(x,t)}{\partial t} &= D_w \frac{\partial^2 \xi(x,t)}{\partial x^2} \\
\frac{\partial \phi(x,t)}{\partial t} &= D_w \frac{\partial^2 \phi(x,t)}{\partial x^2} \\
\frac{\partial c_M^o(x,t)}{\partial t} &= D_o \frac{\partial^2 c_M^o(x,t)}{\partial x^2} \\
\frac{\partial c_{ML}^o(x,t)}{\partial t} &= D_o \frac{\partial^2 c_{ML}^o(x,t)}{\partial x^2}
\end{aligned}\right\} \tag{14}$$

$$\left.\begin{aligned} x \le 0, t = 0 \\ x \to -\infty, t \ge 0 \end{aligned}\right\} \qquad \xi = \mathrm{c}^* = c_M^* + c_{ML}^* \quad ; \quad \phi = 0 \tag{15}$$

$$\left.\begin{aligned} x \ge 0, t = 0 \\ x \to \infty, t \ge 0 \end{aligned}\right\} \qquad \mathrm{c}_M^o = \mathrm{c}_{ML}^o = 0 \tag{16}$$

$$x = 0, t > 0\}$$

$$\left(\frac{\partial \xi}{\partial x}\right)_{x=0} + e^{-\kappa t}\left(\frac{\partial \phi}{\partial x}\right)_{x=0} = (1+K)\frac{D_o}{D_w}\left(\frac{\partial c_M^o}{\partial x}\right)_{x=0} \tag{17}$$

$$K\left(\frac{\partial \xi}{\partial x}\right)_{x=0} - e^{-\kappa t}\left(\frac{\partial \phi}{\partial x}\right)_{x=0} = (1+K)\frac{D_o}{D_w}\left(\frac{\partial c_{ML}^o}{\partial x}\right)_{x=0} \tag{18}$$

$$c_M^o(0) = \frac{\xi(0) + e^{-\kappa t}\phi(0)}{1+K}\mathrm{e}^{\eta_1} \tag{19}$$

$$c_{ML}^o(0) = \frac{K\xi(0) - e^{-\kappa t}\phi(0)}{1+K}\mathrm{e}^{\eta_2} \tag{20}$$

with

$$\kappa = k_1 + k_2 \tag{21}$$

Moreover, the current response is given by

$$I = -zFAD_w\left(\frac{\partial \xi}{\partial x}\right)_{x=0} \tag{22}$$

By following a mathematical procedure analogous to that employed in reference [39], based on Koutecký's dimensionless parameters method [40, 41] (see Appendix B), the following rigorous expression for the current is obtained

$$\frac{I_{\mathrm{rig}}}{I_{\mathrm{d}}}=\frac{\gamma\left[e^{\eta_1}+Ke^{\eta_2}+\gamma e^{\eta_1}e^{\eta_2}\left(1+K\right)+\dfrac{K\gamma\left(e^{\eta_2}-e^{\eta_1}\right)^2}{\left(1+K\right)\left(1+\gamma e^{\eta_1}\right)\left(1+\gamma e^{\eta_2}\right)}S\left(\chi\right)\right]}{\left(1+K\right)\left(1+\gamma e^{\eta_1}\right)\left(1+\gamma e^{\eta_2}\right)} \tag{23}$$

where

$$\gamma=\sqrt{\frac{D_o}{D_w}} \tag{24}$$

I_{d} is the diffusion-limited current of a simple ion transfer process at macrointerfaces [12]

$$I_{\mathrm{d}}=zFAc^{*}\sqrt{\frac{D_w}{\pi t}} \tag{25}$$

and $S\left(\chi\right)$ is given by

$$S\left(\chi\right)=\sum_{j=1}^{\infty}\lambda_j\chi^{j} \tag{26}$$

where

$$\lambda_1=\frac{p_2}{p_0}-1 \tag{27}$$

$$\lambda_j=\frac{1}{j!}\left(\frac{p_{2j}}{p_0}-1\right)-\frac{\gamma}{\left(1+K\right)\left(1+\gamma e^{\eta_1}\right)\left(1+\gamma e^{\eta_2}\right)}\times \sum_{i=1}^{j-1}\frac{\lambda_i}{\left(j-i\right)!}\left[Ke^{\eta_1}+e^{\eta_2}+\gamma e^{\eta_1}e^{\eta_2}\left(1+K\right)+\frac{p_{2\mathrm{j}}}{p_{2\mathrm{i}}}\left(\frac{1+K+\gamma\left[e^{\eta_1}+Ke^{\eta_2}\right]}{\gamma}\right)\right] \qquad j>1 \tag{28}$$

$$\chi=\kappa t \tag{29}$$

with

$$\begin{cases}p_0=\dfrac{2}{\sqrt{\pi}}\\ p_{i>0}=\dfrac{2i}{p_{i-1}}\end{cases} \tag{30}$$

2.1.1 Kinetic steady state aproximation (kss)

When the kinetics of the coupled chemical reaction is fast enough, it is adequate to suppose that the equilibrium perturbation is independent of the electrolysis time [42]

$$\frac{\partial \phi_{ss}}{\partial t} = 0 \tag{31}$$

with ϕ_{ss} being defined as

$$\phi_{ss} = Kc_M^w - c_{ML}^w \tag{32}$$

By taking into account Eqs.(31) and (32), the system (2) leads to the following differential equation for the variable ϕ_{ss}

$$\frac{\partial^2 \phi_{ss}(x)}{\partial x^2} - \frac{\kappa}{D_w}\phi_{ss}(x) = 0 \tag{33}$$

the solution of which is given by

$$\phi_{ss}(x) = \phi_{ss}(0)\mathrm{e}^{\frac{x}{\delta_r}} \tag{34}$$

where $x \le 0$ in the aqueous phase and δ_r is the thickness of the linear reaction layer where the chemical equilibrium is disturbed

$$\delta_r = \sqrt{\frac{D_w}{\kappa}} \tag{35}$$

Thus, by applying Koutecký's dimensionless parameter method and considering Eq.(34) , the expression for the current under the *kss* approach is obtained

$$\frac{I_{\mathrm{kss}}}{I_{\mathrm{d}}} = \frac{\gamma}{Ke^{\eta_1} + e^{\eta_2} + \gamma e^{\eta_1}e^{\eta_2}(1+K)}\left[(1+K)e^{\eta_1}e^{\eta_2} + \frac{K\left(e^{\eta_1} - e^{\eta_2}\right)^2 F(\chi_{kss})}{1+K+\gamma\left(e^{\eta_1} + Ke^{\eta_2}\right)}\right] \tag{36}$$

where

$$F(\chi_{kss}) = \frac{\sqrt{\pi}}{2}\chi_{kss}e^{\left(\frac{\chi_{kss}}{2}\right)^2} erfc\left(\frac{\chi_{kss}}{2}\right) \tag{37}$$

$$\chi_{kss} = \frac{2\sqrt{\chi}\left[1+K+\gamma\left(e^{\eta_1}+Ke^{\eta_2}\right)\right]}{\gamma\left[Ke^{\eta_1}+e^{\eta_2}+\gamma e^{\eta_1}e^{\eta_2}\left(1+K\right)\right]} \tag{38}$$

and χ is defined by Eq.(29). The validity of the approximate solution (36) has been analyzed by comparison with the rigorous one (Eq.(23)), finding that the error decreases as χ increases and $\left|\Delta\phi^{0'}\right|$ decreases. In regard to the influence of K, the error increases as the proportion of the most lipophilic species decreases (i.e. it increases with K if $\Delta\phi^{0'} > 0$ and it decreases if $\Delta\phi^{0'} < 0$). For example, for $0.2 \le K \le 5$ and $\left|\Delta\phi^{0'}\right| \le 200$ mV, both solutions coincide for $\chi \ge 3.2$ with a difference smaller than 5% and for $\chi \ge 14$ with a difference smaller than 1%, independently of the value of γ.

2.1.2 Particular case: only the ion M^{z+} *(or the complex* ML^{z+}*) is transferred*

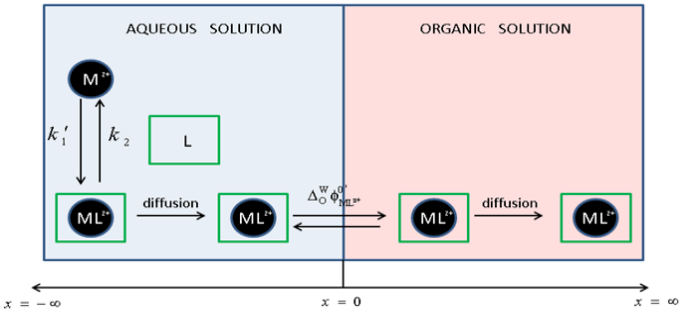

Aqueous complexation followed by transfer (**ACT**)

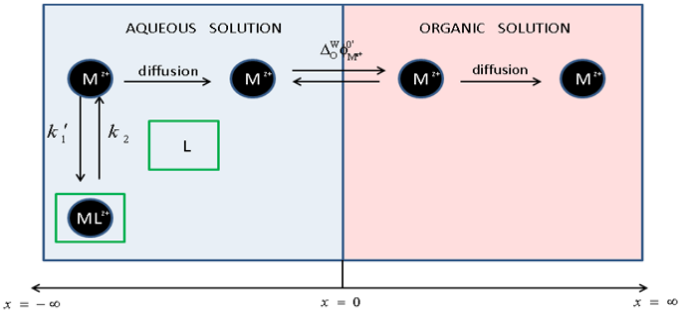

Aqueous dissociation followed by transfer (**ADT**)

Scheme II

Under these conditions, when only the ion is transferred (aqueous dissociation followed by transfer (ADT), see Scheme II), the rigorous expression for NPV can be easily deduced from Eq.(23) by making $\Delta_O^W\phi_{ML^+}^{0'} \to +\infty$ (i.e. $e^{\eta_2} \to 0$)

$$\frac{I_{rig}^{ADT}}{I_d} = \frac{\gamma e^{\eta_1}}{\left(1+K\right)\left(1+\gamma e^{\eta_1}\right)}\left[1+\frac{K\gamma e^{\eta_1}}{\left(1+K\right)\left(1+\gamma e^{\eta_1}\right)}\sum_{j=1}^{\infty}\lambda_j^{ADT}\chi^j\right] \tag{39}$$

with

$$\lambda_1^{ADT} = \frac{p_2}{p_0} - 1 \tag{40}$$

$$\lambda_j^{ADT} = \frac{1}{j!}\left(\frac{p_{2j}}{p_0} - 1\right) - \frac{\gamma}{(1+K)\left(1+\gamma e^{\eta_1}\right)} \sum_{i=1}^{j-1} \frac{\lambda_i}{(j-i)!}\left[Ke^{\eta_1} + \frac{p_{2j}}{p_{2i}}\left(\frac{1+K+\gamma e^{\eta_1}}{\gamma}\right)\right];\ j>1 \tag{41}$$

and p_z being defined in Eq. (30). In addition, from (36) one obtains the *kss* approximate solution for the current

$$\frac{I_{kss}^{ADT}}{I_d} = \frac{\gamma e^{\eta_1} F\left(\chi_{kss}^{M^{z+}}\right)}{1+K+\gamma e^{\eta_1}} \tag{42}$$

where $F\left(\chi_{kss}^{M^{z+}}\right)$ is given by Eq.(37), with

$$\chi_{kss}^{ADT} = \frac{2\sqrt{\chi}\left(1+K+\gamma e^{\eta_1}\right)}{K\gamma e^{\eta_1}} \tag{43}$$

Eqs.(39)-(43) coincide with those reported in previous works for the equivalent CE-mechanisms in electron transfer processes [43, 44]. Analogous expressions for the case where ML^{z+} is the only species transferred (aqueous complexation followed by transfer (ACT), see Scheme II) are also deduced by making $\Delta_O^W \phi_{M^+}^{0'} \to +\infty$ (i.e. $e^{\eta_1} \to 0$) in Eqs.(23) and (36). Such expressions are equivalent to (39)-(43) by replacing η_1 by η_2 and K by $1/K$.

2.2 Total equilibrium conditions (te): application of any voltammetric technique

When the chemical kinetics in the aqueous phase is very fast in comparison with diffusion, we can assume that the chemical equilibrium is maintained at any time and any point in the aqueous solution. Under these conditions, the expression for the current greatly simplifies by making $\chi \to \infty$ ($F\left(\chi_{kss}\right) \to 1$) in Eq.(36), in a such way that it is obtained that

$$\frac{I_{te}}{I_{\mathrm{d}}} = \left[\frac{\gamma\left(\mathrm{e}^{\eta_1} + K\mathrm{e}^{\eta_2}\right)}{1 + K + \gamma\left(\mathrm{e}^{\eta_1} + K\mathrm{e}^{\eta_2}\right)} \right] \tag{44}$$

This equation corresponds to a single wave, the half-wave potential of which is

$$E_{1/2}^{\mathrm{te}} = \Delta_{\mathrm{o}}^{\mathrm{w}}\phi_{\mathrm{ML}^{z+}}^{o'} + \frac{RT}{zF}\ln\left(\frac{1}{\gamma}\right) + \frac{RT}{zF}\ln\left(1+K\right) - \frac{RT}{zF}\ln\left(K + e^{\frac{zF}{RT}\Delta\phi^{0'}}\right) \tag{45}$$

with

$$\Delta\phi^{0'} = \Delta_{\mathrm{O}}^{\mathrm{W}}\phi_{\mathrm{ML}^{z+}}^{0'} - \Delta_{\mathrm{O}}^{\mathrm{W}}\phi_{\mathrm{M}^{z+}}^{0'} \tag{46}$$

Furthermore, the assumption of total equilibrium conditions enables us to derive an analytical expression for the current response when any sequence of *p* potential steps $E_1, E_2, ...E_p$ is applied. Thus, it can be demonstrated that the interfacial concentrations associated with each potential pulse are only dependent on the value of the applied potential and independent of the previous potential pulses. Therefore, the superposition principle can be applied [45] in a such way that the current corresponding to the *p*-th potential step can be written as

$$I_{\mathrm{te,p}} = zFA\sqrt{\frac{D_w}{\pi}}\sum_{i=1}^{p}\frac{c_T^{w,i-1}\left(0\right) - c_T^{w,i}\left(0\right)}{\sqrt{t_{ip}}} \tag{47}$$

where

$$\left.\begin{aligned} c_T^{w,0}\left(0\right) &= c^* \\ c_T^{w,i}\left(0\right) &= \frac{c^*\left(1+K\right)}{1 + K + \gamma\left(e^{\eta_1^{(\mathrm{i})}} + Ke^{\eta_2^{(\mathrm{i})}}\right)} \quad ; \quad i > 0 \end{aligned}\right\} \tag{48}$$

$$t_{i,p} = \sum_{m=i}^{p-1}\tau_m + t_p \tag{49}$$

with

$$\eta_1^{(i)} = \frac{zF}{RT}\left(E_i - \Delta_{\mathrm{O}}^{\mathrm{W}}\phi_{\mathrm{M}^{z+}}^{0'}\right) \quad ; i > 0 \tag{50}$$

$$\eta_2^{(i)} = \frac{zF}{RT}\left(E_i - \Delta_{\mathrm{O}}^{\mathrm{W}}\phi_{\mathrm{ML}^{z+}}^{0'}\right) \quad ; i > 0 \tag{51}$$

Note that the general solution (47) can be applied to any voltammetric technique. For example, the normalized expressions for staircase cyclic voltammetry (SCV) and square wave voltammetry (SWV) are as follows

$$\begin{aligned}\Psi_{te,SCV} &= \frac{I_{SCV}}{zFAc^*\sqrt{aD_w}} \\ &= \sqrt{\frac{RT}{\pi F \Delta E}}(1+K)\sum_{i=1}^{p}\frac{G(\eta_{i-1}) - G(\eta_i)}{\sqrt{p-i+1}}\end{aligned} \tag{52}$$

$$\begin{aligned}\Psi_{te,SWV} &= \frac{\Delta I_{SWV}\sqrt{\tau}}{zFAc^*\sqrt{D_w}} \\ &= \frac{1+K}{\sqrt{\pi}}\left[\sum_{i=1}^{2p-1}\left\{\left(G(\eta_{i-1}) - G(\eta_i)\right)\left(\frac{1}{\sqrt{2p-i}} - \frac{1}{\sqrt{2p-i+1}}\right)\right\} + G(\eta_{2p}) - G(\eta_{2p-1})\right]\end{aligned} \tag{53}$$

where ΔE is the pulse step in SCV (with $\Delta E \le 0.01$ mV the cyclic voltammogram (CV) is obtained [46]) and τ is the duration of each applied potential in SWV (the frequency is defined as $f = 1/2\tau$). Moreover, $G(\eta_i)$ and a are given by

$$\left.\begin{aligned} G(\eta_0) &= \frac{1}{1+K} \\ G(\eta_i) &= \frac{1}{1+K+\gamma\left(e^{\eta_1^{(i)}} + Ke^{\eta_2^{(i)}}\right)} \quad ; \quad i > 0 \end{aligned}\right\} \tag{54}$$

$$a = \frac{Fv}{RT} \tag{55}$$

with v being the scan rate in CV.

2.2.1 Particular case: only the ion M^{z+} *(or the complex* ML^{z+}*) is transferred*

Under these conditions, by making $e^{\eta_2} \to 0$ in Eqs. (44)-(45), the NPV current and the half wave potential when only the free ion is transferred (ADT mechanism) are given by

$$\frac{I_{te}^{ADT}}{I_d} = \frac{\gamma e^{\eta_1}}{1 + K + \gamma e^{\eta_1}} \tag{56}$$

$$E_{1/2}^{te,ADT} = \Delta_o^w \phi_{M^{z+}}^{o'} + \frac{RT}{zF} \ln\left(\frac{1}{\gamma}\right) + \frac{RT}{zF} \ln(1+K) \tag{57}$$

Moreover, the general solution (47) for an arbitrary sequence of potentials can also be used in this particular case, by making $e^{\eta_2} \to 0$ in the expressions of the surface concentrations (Eq.(48)). Hence, the CV and SWV responses are also given by Eqs. (52)-(53) with

$$\left.\begin{aligned} G^{ADT}(\eta_0) &= \frac{1}{1+K} \\ G^{ADT}(\eta_i) &= \frac{1}{1+K+\gamma e^{\eta_1^{(i)}}} \quad ; \quad i > 0 \end{aligned}\right\} \tag{58}$$

Analogous expressions for the case where ML^{z+} is the only species transferred (ACT mechanism) are also deduced by making $\Delta_O^W \phi_{M^+}^{0'} \to +\infty$ (i.e. $e^{\eta_1} \to 0$) in Eqs.(44)-(45), (48) and (54). Such expressions are equivalent to (52)-(53) and (56)-(58) by replacing $\Delta_o^w \phi_{M^{z+}}^{o'}$ by $\Delta_o^w \phi_{ML^{z+}}^{o'}$ (η_1 by η_2) and K by $1/K$.

3. RESULTS AND DISCUSSION

3.1. Chemical kinetics: normal pulse voltammetry (NPV), differential voltammetry (dNPV) and chronoamperometry

The effect of the chemical kinetics on the NPV voltammograms is parameterized here by the variable χ, defined as $\chi = \kappa t$ (Eq.(29)). The increment of the chemical rate constant κ ($\kappa = k_1 + k_2$) or the duration τ of the potential pulse ($0 \le t \le \tau$) results in higher values of χ. Therefore, the "effective" chemical kinetics can be varied experimentally by changing the duration of the applied potentials. Note that this is qualitatively equivalent to changing the scan rate in cyclic voltammetry and the frequency in square wave voltammetry. Thus, the decrease of the scan rate in CV or the frequency in SWV is analogous to the use of longer pulse times in NPV. Furthermore, the value of κ can also be modified by means of the initial concentration of ligand (c_L^*), since $k_1 = k_1' c_L^*$.

The influence of χ is analysed in Figs. 1 and 2, where NPV-voltammograms are plotted for a ratio of diffusion coefficients $D_o / D_w = 0.001$. Note that this large difference between the diffusivity of the ionic species in phases *w* and *o* is not uncommon in the present context given than 2- and even 3-order-of-magnitude differences have been reported between the *D*-values in conventional solvents and solvent polymeric membranes or room temperature ionic liquids [11, 36-38]. An apparent equilibrium constant *K* = 2 is considered (that is, $c_M^* = c^*/3$ and $c_{ML}^* = 2c^*/3$) and several values of the difference between the formal ion transfer potentials ($\Delta\phi^{0'} = \Delta_O^W \phi_{ML^{z+}}^{0'} - \Delta_O^W \phi_{M^{z+}}^{0'}$), taking into account that the transfer of the complex can be thermodynamically less favourable ($\Delta\phi^{0'} > 0$, Fig. 1) or more favourable ($\Delta\phi^{0'} < 0$, Fig. 2) than the transfer of the free species.

As can be seen in Figs. 1A and 2A, when the difference $\Delta\phi^{0'}$ is large $\left(\left|\Delta\phi^{0'}\right| = 200\text{mV}\right)$ and two waves can be distinguished, the first signal is related to the transfer of the most lipophilic species, *i.e.* the species with less positive formal transfer potential (M^{z+} in Fig.1A and ML^{z+} in Fig.2A). Hence, the limiting current of the first wave (I_{lim}^{1}) is larger in Fig. 2A than in Fig. 1A since initially ML^{z+} is present in a higher concentration according to the chemical equilibrium constant considered ($c_{ML}^{*} = 2c_{M}^{*}$). As the χ-value is higher, the magnitude of the first wave increases. This can be understood by the faster interconversion between M^{z+} and ML^{z+}. As discussed in Section 2.1.2, under the $\Delta\phi^{0'}$-values in Figs. 1A and 2A, the limiting current of the first wave (I_{lim}^{1}) and their half-wave potential ($E_{1/2}^{1}$) are identical to those obtained for the equivalent CE-mechanism (Eqs. (39)-(43)) with the species transferred being M^{z+} in Fig.1A and ML^{z+} in Fig.2A.

The voltammograms also undergo a transition from a double wave to a single one as the χ-value is increased. In the limit of very fast kinetics, they coincide with the response predicted under total equilibrium conditions (grey line, Eq.(44)), the limiting current of the wave being proportional to the sum of the initial concentrations of species M^{z+} and ML^{z+} in water (c^{*}). On the other hand, when the value of χ is small ($\chi \leq 0.01$), the voltammograms show two waves corresponding to the "independent" transfer of each species, which are centred on the corresponding half-wave potential given by [14]

$$E_{1/2,j} = \Delta_{\text{O}}^{\text{W}}\phi_{j}^{0'} + \frac{RT}{zF}\ln\left(\frac{1}{\gamma}\right) \quad (j = M^{z+}, ML^{z+}) \tag{59}$$

Note that the variation of the signal shape with the pulse duration is a simple criterion to discriminate between the mechanism depicted in Scheme I and the situation where there

is no interconversion between species M^{z+} and ML^{z+}, that is, the chemical process does not take place (at least within the voltammetric time-scale). Also note that the above conclusions are qualitatively applicable to other voltammetric techniques and the corresponding current-potential curves have an analogous behaviour as the time-scale of the experiment is changed.

The value of the difference $\Delta\phi^{0'}$ also has an effect on the NPV-voltammograms, as shown in Figs. 1B, 1C, 2B and 2C. Thus, smaller differences between the formal transfer potentials give rise to the overlapping of the two waves. Hence, the effect of the chemical kinetics is less apparent and so more difficult to detect experimentally. The response finally turns into a single signal when $\Delta\phi^{0'} \to 0$ (see Figs. 1C and 2C), which is insensitive to the χ-value since under these conditions it is fulfilled that $\eta_1 = \eta_2 = \eta$ (see Eqs.(9) and (10)) in a such way that Eq.(23) leads to the following expression for the current-potential response:

$$\frac{I_{\Delta E^0=0}}{I_d} = \frac{\gamma e^{\eta}}{1+\gamma e^{\eta}} \tag{60}$$

which corresponds to a single sigmoidal curve (Figs. 1C and 2C). As can be inferred from Eq. (60), the current is independent of the chemical reaction since both species have identical lipophilicity and they are transferred at the same potential ($\Delta_O^W\phi^{0'}_{M^{z+}} = \Delta_O^W\phi^{0'}_{ML^{z+}}$). In fact, the above expression coincides with that obtained for an ion transfer reaction without any kinetic constraints in the aqueous phase [14].

The effect of the equilibrium constant is showed in Fig.3, for $\Delta\phi^{0'}$ = 200 mV and $D_o / D_w = 0.001$ (note that the conclusions are qualitatively analogous for any other values of $\Delta\phi^{0'}$ and D_o / D_w). As expected, when $K \gg 1$ or $K \ll 1$ the curves tends to those corresponding to the simple transfer of the complex or the free species,

respectively, given that under such conditions they are practically the only species present in the aqueous medium. On the other hand, two waves are obtained for non-extreme values of *K* when total equilibrium conditions are not achieved (Figs. 3A and 3B). As can be seen, lower *K*-values result in a higher limiting current of the first signal ($I_{\lim}^{1}$), due to the increment of the initial concentration of the most lipophilic species M^{z+}. The variation of the limiting current with *K* is less notorious for large κ-values, since the chemical reaction provides a higher amount of species M^{z+}. Note that even if the initial concentration of the most lipophilic species is not very large in solution (e.g. *K* = 10 in Fig. 3B), its corresponding electrochemical signal can be significant if the interconversion $ML^{z+} \rightleftarrows M^{z+}$ is fast. This point is important for the correct interpretation of electrochemical signals in speciation studies.

For large χ-values such that total chemical equilibrium conditions are attained (Fig. 3C), a single curve is obtained independently of the values of *K* and $\Delta\phi^{0'}$ (see also Figs.1 and 2) according to Eq.(44), the position of which is given by Eq.(45). Thus, the voltammogram shifts towards more positive potentials as the equilibrium constant takes larger values, since the proportion of the less lipophilic species (*i.e.*, the complexed species in this figure) increases with *K* (see Eq.(1)).

The effect of the variation of the concentration of species L (c_L^*) is showed in Fig.4. The value of c_L^* modifies the value of both the *apparent* equilibrium constant ($K = K_c c_L^*$) and the "effective" rate constant of complexation ($k_1 = k_1' c_L^*$), in a such way that both *K* and k_1 increase with c_L^*. Taking the above two effects into account, NPV-curves have been plotted in Fig. 4.A for different concentrations of ligand (assuming that c_L^* is in a large excess with respect to c^* in all the cases) and K_c = 10 M^{-1} (

$K_c = k_1'/k_2$). As can be seen, given that $\Delta\phi^{0'} > 0$ (*i.e.*, $\Delta_O^W\phi_{ML^{z+}}^{0'} > \Delta_O^W\phi_{M^{z+}}^{0'}$), higher concentrations of the ligand result in a lower limiting current of the first wave (I_{lim}^1) and the shift of the voltammogram towards more positive potentials. This is a consequence of the increase of the concentration of species ML^{z+}, which has been considered to be less lipophilic than M^{z+} (the opposite behaviour would be observed if ML^{z+} were the most lipophilic species). Obviously, the voltammograms would be insensitive to the value of c_L^* in the absence of the homogeneous chemical reaction (*i.e.*, $\chi \ll 1$).

The study of the variation of the position of the signal and of the value of I_{lim}^1 (provided that the difference of formal transfer potentials is large enough) can be used to determine the rate and equilibrium constants. In Figs. 4B and 4C, the variation of I_{lim}^1 and the position of the signal (parameterized by means of the potential E_{half} at which the normalized current takes the value $I/I_d = 0.5$) with c_L^* have been plotted for different values of k_1' and k_2, maintaining the ratio k_1'/k_2 (= K_c) constant. The shape of the curves is very similar for any K_c value, the influence of which is the shift of the curve towards smaller c_L^*-values as K_c increases (not shown). The rate constants and the real equilibrium constant can be extracted by fitting the variation of I_{lim}^1 and E_{half} with c_L^* within the adequate range of ligand concentrations ($K_c c_L^*$ approximately between 1 and 10). The two limit values of the curves in Figs. 4B correspond to the half-wave potentials of species M^{z+} (very small ligand concentration) and ML^{z+} (very high ligand concentration), which are given by Eq.(59). Therefore, when the range of c_L^* is not limited by the nature of the ligand and/or by its solubility, the half-wave potentials of the ion transferred can be determined directly from these two limit values.

The theory developed for the ACDT mechanism depicted in Scheme I also allows us to study the current-potential response in derivative voltammetry (dNPV), obtained by differentiation of the experimental NPV curve. A notable advantage of this technique is the higher resolution that it offers when the signals are overlapped. In Fig. 5A, the influence of χ on the dNPV-voltammograms is shown for $\Delta\phi^{0'}$ = 200mV. As discussed from the NPV curves, the increment of χ leads to the transition of the signal from two peaks centred at the corresponding half-wave potentials to a single peak. The latter coincides with the response obtained under total equilibrium conditions (grey line) with E_{peak} being given by Eq.(45). Furthermore, the peak current of the first signal increases with χ whereas the second peak undergoes the opposite behaviour. Note that the two peak potentials take more positive values as the chemical interconversion is faster.

The influence of the equilibrium constant on the dNPV response is examined in Fig. 5B, for $\Delta\phi^{0'}$ = 200mV and χ = 1. In this case the effect is also analogous to that observed in NPV (see Fig. 3A). Thus, the voltammograms show two peaks when *K* takes intermediate values, the magnitude of the first one (transfer of M^{z+}) decreasing with *K* whereas the second signal increases as *K* is larger. In addition, the two peaks converge into a single one when $K \to \infty$ (simple transfer of species ML^{z+}) or $K \to 0$ (simple transfer of species M^{z+}). This figure illustrates the idea mentioned above that the conclusions reached for the NPV signal are qualitatively applicable to other voltammetric techniques.

Let us move now to the study of the chronoamperometric response; *i.e.* the current-time curves (*I vs t*) obtained under the application of a constant potential. In Fig. 6, the influence of the chemical kinetics and of the equilibrium constant on the *I-t* response is analyzed for $\Delta\phi^{0'} = 200$ mV, upon the application of a potential

($E - \Delta_{\mathrm{O}}^{\mathrm{W}}\phi_{M^{z+}}^{0'} = 200\,\mathrm{mV}$) that corresponds to the limiting current of the first wave of the NPV curve (see Fig. 1A).

With regard to the effect of κ (Fig.6A), one can observe that the increment of this variable results in larger values of the current, reaching the limit of total equilibrium for very fast kinetics (see inset in Fig.6A). Thus, the plot of $I_{\mathrm{lim}}^{1} / I_d$ versus χ is a sigmoid with two limit values corresponding to the simple transfer of species M^{z+} (lower limit, slow chemical kinetics) and the ion transfer under total equilibrium conditions (upper limit, fast chemical kinetics). The position of this sigmoid is a function of the *K*-value, since it determines the initial concentrations of each species and so the value of current obtained (the smaller the apparent equilibrium constant, the higher the current measured).

The effect of *K* is shown in Figs. 6B and 6C, where the current density-time curves are plotted for two different values of κ and several *apparent* equilibrium constants (indicated on the graphs). As can be observed, the decrease of *K* leads to higher values of the current density, according to the increase of the initial concentration of the free species. Moreover, for a fixed value of *K*, the current density takes larger values as κ increases, since the chemical reaction is able to provide a larger amount of species M^{z+}. Note that the plots $I_{\mathrm{lim}}^{1} / I_d$ *vs* t are constants when $K \to 0$ or $K \to \infty$, since under these conditions there is practically a single species present in the aqueous medium and the chronoamperogram follows a Cottrelian behaviour [12]. Thus, $I_{\mathrm{lim}}^{1} / I_d \approx 1$ for very small *K*-values ($c_M^* = c^*$) and $I_{\mathrm{lim}}^{1} / I_d \approx 0$ for extremely high *K*-values ($c_M^* = 0$). On the other hand, deviations from the Cottrell equation are observed for intermediate values of *K* (Figs. 6B and 6C) and κ (Fig. 6A).

3.2. Total equilibrium conditions: cyclic voltammetry (CV) and square wave voltammetry (SWV)

As discussed in Section 2.3, under total equilibrium conditions (very fast kinetics), an analytical equation can be obtained for any voltammetric technique (Eq.(47)), such as cyclic voltammetry (CV) and square wave voltammetry (SWV). In Figs. 7A and 7B, the influence of the scan rate (v) in CV and of the frequency (f) in SWV are shown. Unlike the cases in Fig. 1 (under the influence of the chemical kinetics), the time scale of the experiment has no influence on the shape of the voltammograms. The only effect of v and f is the increment of the peak current whereas the position and shape of the signal are not altered. Note that this effect is also observed when there are no chemical reactions coupled to the ion transfer processes [12, 13, 47], such that, as expected, the variation of the response with the experimental time-scale cannot be used to detect the occurrence of the chemical reaction.

The presence of the coupled chemical process can be probed by varying the bulk concentration of ligand c_L^*. In Figs. 7C and 7D, one can observe that the only influence of the c_L^*-value on the CV and SWV-voltammograms under total equilibrium conditions is the shift of the voltammograms. For $\Delta\phi^{0'} > 0$ (*i.e.* the complex is less lipophilic than the free species) the shift takes place towards more positive potentials as c_L^* is increased, whereas the shape of the response is not affected (compare with the results shown in Fig. 4A). This is a consequence of the very fast kinetics of interconversion between M^{z+} and ML^{z+}, such that the presence of ligand only influences the value of the *apparent* equilibrium constant *K*. Obviously, the shift of the voltammograms would take place towards less positive potentials if ML^{z+} were the most lipophilic ionic species ($\Delta\phi^{0'} < 0$, not shown) and the position of the signal would remain unaffected if

there were not any coupled chemical reaction. Therefore, the variation of the signal with c_L^* is a direct and straightforward way to detect the presence of the chemical process as well as to distinguish the degree of lipophilicity of the two ionic species.

Variable c_L^*-experiments can also be performed to quantify the value of the real equilibrium constant K_c. The shift of the voltammograms can be quantified through the values of the peak potential of the forward peak in CV ($E_{\text{p,forward}}^{\text{CV}}$) and the peak potential in SWV ($E_{\text{peak}}^{\text{SWV}}$). The latter coincides with the half-wave potential under equilibrium conditions [48] (Eq.(45)), whereas the forward peak potential in CV differs from this by ≈ 28.5 mV at 25ºC for $z=1$ [12]:

$$\left.\begin{aligned} E_{\text{peak}}^{\text{SWV}} - E_{1/2,M^{z+}} &= \Delta\phi^{0'} - \frac{RT}{zF}\ln\left(\frac{K_c c_L^* + e^{\frac{zF}{RT}\Delta\phi^{0'}}}{1+K_c c_L^*}\right) \\ E_{\text{p,forward}}^{\text{CV}} - E_{1/2,M^{z+}} &= \Delta\phi^{0'} - \frac{RT}{zF}\ln\left(\frac{K_c c_L^* + e^{\frac{zF}{RT}\Delta\phi^{0'}}}{1+K_c c_L^*}\right) + 1.109\frac{RT}{zF} \end{aligned}\right\} \quad (61)$$

with $E_{1/2,M}$ being defined by Eq.(59). By fitting the variations of the peak potentials with the ligand concentration (see Figs. 7E and 7F) one can determine K_c and the difference between the half-wave potentials (which coincides in this case with the difference between the formal transfer potentials). Note that according to Eqs. (61) the influence of the coupled chemical reaction on the position of the signal depends on the charge of the free and complexed ions (*z*).

Finally, the influence of the charge of the ionic species is analyzed in Fig. 8. Fig. 8A shows that the forward peak current in CV is affected by *z*, such that $I_{p,\,forward}^{CV}$ is proportional to $|z|^{3/2}$, as described for single charge transfer processes (the Randles-Sevckic equation [12]). Thus, the ratio between the slopes of the two plots depicted in Fig.

8A is $2^{3/2}$ (= 2.8). In addition, the peak-to-peak separation for z = 2 (≈ 29 mV) is half of that corresponding to z = 1 (≈ 58 mV), as it is also well-known for simple charge transfer processes [12].

Regarding the effect in SWV, one can observe that the peak current increases with the ion charge z (Fig. 8B). Indeed, the peak current is a function of the product $|z|E_{sw}$ (with E_{sw} being the square wave amplitude), in a such way that for a given $|z|E_{sw}$-value the same value of $\left|I_{peak}^{SWV}/z\right|$ is obtained [47] (see grey lines in Fig. 8B). The half-peak width ($W_{1/2}$) of the SWV-curve is also a function of the charge of the ions (Fig. 8C). These $W_{1/2}$-values have been calculated from the following equation reported for a simple ion transfer [49] that, as expected from Eq. (53), also describes the ACDT mechanism under total equilibrium conditions:

$$W_{1/2} = \frac{RT}{|z|F}\ln\left[\frac{1+e^{2\eta_{sw}}+4e^{\eta_{sw}}+\sqrt{\left(1+e^{2\eta_{sw}}+4e^{\eta_{sw}}\right)^2-4e^{2\eta_{sw}}}}{1+e^{2\eta_{sw}}+4e^{\eta_{sw}}-\sqrt{\left(1+e^{2\eta_{sw}}+4e^{\eta_{sw}}\right)^2-4e^{2\eta_{sw}}}}\right] \tag{62}$$

where

$$\eta_{sw} = \frac{|z|F}{RT}E_{sw} \tag{63}$$

Therefore, the half-peak width is a function of $|z|$ and $|z|E_{sw}$ such that equal $|z|E_{sw}$ values lead to the same value of $|z|W_{1/2}$ [47] (see grey lines in Fig. 8C). As can be observed in Fig. 8C, $W_{1/2}(z=1)/W_{1/2}(z=2) \approx 2$ when the value of the amplitude is small but this ratio tends to unity as E_{sw} takes higher values.

4. CONCLUSIONS

Analytical explicit equations have been reported for the response in different voltammetric techniques of two ionic species that interconvert through a chemical reaction and both can be transferred from water to an organic solution, solvent polymeric membrane or ionic liquid (the ACDT mechanism). Rigorous and approximate explicit solutions are presented for normal pulse voltammetry (NPV), derivative voltammetry (dNPV) and chronoamperometry including the effects of the chemical kinetics and also of the likely different diffusion coefficients in each phase. Moreover, a general expression has also been obtained for any voltammetric technique when the chemical kinetics is very fast (chemical equilibrium conditions).

The above equations enable us to study the variation of the features of the electrochemical response with the time scale of the experiment and with the concentration of ligand for any value of the difference between the formal transfer potentials of the free and complexed species. Different criteria and procedures have been proposed for the detection of the chemical process coupled to the ion transfers, as well as for the determination of the equilibrium and rate constants and the lipophilic character and charge of both ionic species. Thus, the theory reported here enables the rigorous analysis of the dynamic aspects of chemical speciation in voltammetric studies as well as deeper understanding of the voltammetric response and the different physicochemical processes behind it (heterogeneous charge transfer, mass transport and chemical interconversion).

Acknowledgements

The authors greatly appreciate the financial support provided by the Fundación Séneca de la Región de Murcia under the Projects 19887/GERM/15 and 18968/JLI/13. EL also thanks the Ministerio de Economia y Competitividad for the fellowship awarded “Juan de la Cierva – Incorporación 2015” and JMO for the grant received under the Project CTQ2012-36700, co-funded by the European Regional Development Fund.

Appendix A. Symbols

A interfacial area

c^* initial total concentration in the aqueous solution ($c^* = c_M^* + c_{ML}^*$)

c_i^α concentration profile of species *i* (*i* = M, ML, L,) in the phase α ($\alpha = w,m$) under the application of a constant potential

c_i^* bulk concentration of species *i* (*i* = M, ML, L)

$c_T^{w,j}(0)$ total surface concentration in the aqueous solution associated with the *j*-th potential pulse applied in multipulse techniques, under the assumption of total equilibrium conditions ($c_T^{w,j}(0) = c_M^{w,j}(0) + c_{ML}^{w,j}(0)$)

D_i^α diffusion coefficient of species *i* (*i* = M, ML) in phase α ($\alpha = w,m$)

D_α diffusion coefficient in phase α ($\alpha = w,m$)

E applied potential in normal pulse voltammetry (NPV) and chronoamperometry

E_j applied potential in the *j*-th potential pulse in multipulse techniques

$E_{1/2}^1$ half-wave potential of the first wave in NPV

$E_{1/2,i}$ half-wave potential of the simple ion transfer of species *i* (*i* = M, ML)

$E_{1/2}^{te}$ half-wave potential under the assumption of total equilibrium conditions

$E_{1/2}^{te,ADT}$ half-wave potential under the assumption of total equilibrium conditions when M^{z+} is the only species transferred

E_{half} potential at which the NPV-current takes half of its maximum value ($I / I_d = 0.5$)

$E_{p,forward}^{CV}$ forward peak potential in cyclic voltammetry (CV)

E_{peak}^{SWV} peak potential in square wave voltammetry (SWV)

E_s potential step of the staircase in SWV

E_{sw} square wave amplitude in SWV

f SW frequency

F Faraday constant

I current response in NPV

I_{CV} current response in CV

I_d diffusion-limited current of a single transfer process of an ion at concentration c^*

I_{kss} solution for the current response in NPV under the *kss* approach

I_{kss}^{ADT} solution for the current response in NPV under the *kss* approach when M^{z+} is the only species transferred

$I_{\Delta E^0=0}$ solution for the NPV response when M^{z+} and ML^{z+} have the same lipophilicity

$I_{\lim}^{1}$ limiting current of the first wave obtained in NPV for $\left|\Delta\phi^{0'}\right| > 120$ mV

$I_{p,forward}^{CV}$ forward peak current in CV

I_{peak}^{SWV} peak current in SWV

I_{rig} rigorous solution for the current response in NPV

I_{rig}^{ADT} rigorous solution for the current response in NPV when M^{z+} is the only species transferred

I_{te} solution for the current response in NPV under the assumption of total equilibrium conditions

I_{te}^{ADT} solution for the current response in NPV under the assumption of total equilibrium conditions when M^{z+} is the only species transferred

$I_{te,j}$ current associated with the *j*-th potential pulse applied in multipulse techniques, under the assumption of total equilibrium conditions

k_1' forward rate constant of the complexation reaction (M^{-1} s^{-1})

k_1 *effective* forward rate constant of the complexation reaction (s^{-1}) ($k_1 = k_1' c_L^*$)

k_2 backward rate constant of the complexation reaction (s^{-1})

K_c equilibrium constant based on concentrations (M^{-1}) $\left(K_c = \frac{c_{ML}^*}{c_M^* c_L^*} = \frac{k_1'}{k_2} \right)$

K *apparent* equilibrium constant of complexation $\left(K = \frac{c_{ML}^*}{c_M^*} = \frac{k_1' c_L^*}{k_2} \right)$

R molar gas constant

t electrolysis time

T absolute temperature

v scan rate in CV

$W_{1/2}$ half-peak width of the square wave voltammogram

x distance to the interface

z electrical charge of species M^{z+} and ML^{z+}

δ_r thickness of the linear reaction layer

ΔE pulse step in NPV and CV

ΔI_{SWV} current response in SWV

$\Delta_O^W \phi_i^{0'}$ formal ion transfer potential of species i (i = M^{z+}, ML^{z+})

$\Delta\phi^{0'} \left(= \Delta_O^W \phi_{ML^{z+}}^{0'} - \Delta_O^W \phi_{M^{z+}}^{0'} \right)$ difference between the formal transfer potentials of species M^{z+} and ML^{z+}

κ effective chemical rate constant ($\kappa = k_1 + k_2$)

ξ sum of the concentrations of the free and complexed ions in the aqueous solution as a function of time and distance to the interface ($\xi = c_M^w + c_{ML}^w$)

τ duration of each potential applied in NPV and in SWV

τ_j duration of the *j*-th potential pulse applied in multipulse techniques

ϕ perturbation of the chemical equilibrium ($\phi = \left(Kc_M^w - c_{ML}^w \right) e^{(k_1+k_2)t}$)

ϕ_{ss} perturbation of the chemical equilibrium under kinetic steady state conditions $\left(\phi_{ss} = Kc_M^w - c_{ML}^w \right)$

ψ_{CV} normalized SCV signal $\left(\psi_{SCV} = \frac{I_{SCV}}{zFAc^* \sqrt{aD_w}} \right)$

ψ_{SWV} normalized SWV signal $\left(\psi_{SWV} = \frac{\Delta I_{SWV} \sqrt{\tau}}{zFAc^* \sqrt{D_w}} \right)$

χ *effective* chemical kinetics ($\chi = \kappa t$)

Appendix B

In order to solve the equation system (14), the following changes of variables are made

$$\begin{cases} s_\alpha = \dfrac{x}{2\sqrt{D_\alpha t}} \quad ; \quad \alpha = w, o \\ \chi = \kappa t \end{cases} \tag{B1}$$

with $x < 0$ for the aqueous phase (w) and $x < 0$ for the organic solution (o). Thus, the system (14) and the conditions (15)-(20) become

$$\begin{cases} \dfrac{\partial^2 \phi}{\partial s_w^2} + 2s_w \dfrac{\partial\, \phi}{\partial s_w} - 4\chi \dfrac{\partial\, \phi}{\partial \chi} = 0 \\ \dfrac{\partial^2 \xi}{\partial s_w^2} + 2s_w \dfrac{\partial\, \xi}{\partial s_w} - 4\chi \dfrac{\partial\, \xi}{\partial \chi} = 0 \\ \dfrac{\partial^2 c_M^o}{\partial s_o^2} + 2s_o \dfrac{\partial\, c_M^o}{\partial s_o} - 4\chi \dfrac{\partial\, c_M^o}{\partial \chi} = 0 \\ \dfrac{\partial^2 c_{ML}^o}{\partial s_o^2} + 2s_o \dfrac{\partial\, c_{ML}^o}{\partial s_o} - 4\chi \dfrac{\partial\, c_{ML}^o}{\partial \chi} = 0 \end{cases} \tag{B2}$$

$s_w \to -\infty\}$ $\qquad \phi = 0 \;\; ; \;\; \xi = c^*$ (B3)

$s_o \to \infty\}$ $\qquad c_M^o = c_{ML}^o = 0$ (B4)

$s_w = s_o = 0\}$

$$\left(\frac{\partial \xi}{\partial s_w}\right)_{s_w=0} + e^{-\chi}\left(\frac{\partial \phi}{\partial s_w}\right)_{s_w=0} = (1+K)\gamma\left(\frac{\partial c_M^o}{\partial s_o}\right)_{s_o=0} \tag{B5}$$

$$K\left(\frac{\partial \xi}{\partial s_w}\right)_{s_w=0} - e^{-\chi}\left(\frac{\partial \phi}{\partial s_w}\right)_{s_w=0} = (1+K)\gamma\left(\frac{\partial c_{ML}^o}{\partial s_o}\right)_{s_o=0} \tag{B6}$$

$$c_M^o(0) = \frac{\xi(0) + e^{-\chi}\phi(0)}{1+K} e^{\eta_1} \tag{B7}$$

$$c_{ML}^o(0) = \frac{K\xi(0) - e^{-\chi}\phi(0)}{1+K} e^{\eta_2} \tag{B8}$$

According to Koutecký's method [40, 41], the solutions $\phi(x,t)$, $\xi(x,t)$, $c_M^{o}(x,t)$ and $c_{ML}^{o}(x,t)$ are given by

$$\begin{cases} \phi(x,t) = \phi(s_w,\chi) = \sum_{j=0}^{\infty} \alpha_j(s_w)\chi^j \\ \xi(x,t) = \xi(s_w,\chi) = \sum_{j=0}^{\infty} \beta_j(s_w)\chi^j \\ c_M^{o}(x,t) = c_M^{o}(s_o,\chi) = \sum_{j=0}^{\infty} \sigma_j(s_o)\chi^j \\ c_{ML}^{o}(x,t) = c_{ML}^{o}(s_o,\chi) = \sum_{j=0}^{\infty} \delta_j(s_o)\chi^j \end{cases} \tag{B9}$$

that introduced in (B2) lead to the following set of homogeneous differential equation system in a single variable s_α $(\alpha = w,o)$

$$\begin{cases} \alpha_j''(s_w) + 2s_w\alpha_j'(s_w) - 4j\alpha_j(s_w) = 0 \\ \beta_j''(s_w) + 2s_w\beta_j'(s_w) - 4j\beta_j(s_w) = 0 \\ \sigma_j''(s_o) + 2s_o\sigma_j'(s_o) - 4j\sigma_j(s_o) = 0 \\ \delta_j''(s_o) + 2s_o\delta_j'(s_o) - 4j\delta_j(s_o) = 0 \end{cases} \tag{B10}$$

The functions which are solutions of the system (B10) have the following form

$$\left.\begin{aligned} \alpha_j(s_w) &= a_j\psi_{2j}(s_w) + \frac{\alpha_j(s_w \to -\infty)}{\lim_{s_w\to-\infty} L_{2j}} L_{2j} \\ \beta_j(s_w) &= b_j\psi_{2j}(s_w) + \frac{\beta_j(s_w \to -\infty)}{\lim_{s_w\to-\infty} L_{2j}} L_{2j} \\ \sigma_j(s_o) &= c_j\psi_{2j}(s_o) + \frac{\sigma_j(s_o \to \infty)}{\lim_{s_o\to\infty} L_{2j}} L_{2j} \\ \delta_j(s_o) &= d_j\psi_{2j}(s_o) + \frac{\delta_j(s_o \to \infty)}{\lim_{s_o\to\infty} L_{2j}} L_{2j} \end{aligned}\right\} \quad \forall j \tag{B11}$$

where a_j, b_j, c_j and d_j are constants that are determined by application of the boundary value problem, L_{2j} are numeric series of *s* potencies and ψ_i are Koutecký's functions [40, 41, 50]

The initial and bulk conditions (Eqs. (B3)-(B4)) establish that

$$\left.\begin{array}{l}\beta_0(-\infty)=c^*;\quad \beta_{j>0}(-\infty)=0\\ \alpha_j(-\infty)=0\\ \sigma_j(\infty)=0\\ \delta_j(\infty)=0\end{array}\right\}\quad \forall j \tag{B12}$$

in a such way that by taking into account that the function e^{χ} can be expressed as

$$e^{\chi}=\sum_{k=0}^{\infty}\frac{\chi^k}{k!} \tag{B13}$$

the surface conditions (Eqs. (B5)-(B8)) are transformed as follows

$$b_0=a_0\frac{1+K(1+\gamma e^{\eta_1})+\gamma e^{\eta_2}}{K\gamma\left(e^{\eta_2}-e^{\eta_1}\right)};\quad a_0=\frac{Kc^*\gamma\left(e^{\eta_2}-e^{\eta_1}\right)}{(1+K)(1+\gamma e^{\eta_1})\left(1+\gamma e^{\eta_2}\right)}$$

$$\text{for } j>0\ \begin{cases} a_j=\dfrac{p_0a_0}{j!\,p_{2j}}-\dfrac{Ke^{\eta_1}+e^{\eta_2}+\gamma e^{\eta_1}e^{\eta_2}(1+K)}{e^{\eta_2}-e^{\eta_1}}\displaystyle\sum_{i=1}^{j}\frac{p_{2i}b_i}{(j-i)!\,p_{2j}} \\ a_j=\dfrac{a_0}{j!}+\dfrac{1+\gamma e^{\eta_1}+K(1+\gamma e^{\eta_2})}{\gamma\left(e^{\eta_2}-e^{\eta_1}\right)}\displaystyle\sum_{i=1}^{j}\frac{b_i}{(j-i)!}\end{cases} \tag{B14}$$

According to Eq. (22), for the final expression of the current we are only interested in coefficients b_j included in functions β_j (Eq. (B11)) corresponding to the variable ξ (Eq. (B9)), which are obtained by equating the last two equations in (B14):

$$\text{for } j>0:$$

$$b_j=-\frac{\gamma\left(e^{\eta_2}-e^{\eta_1}\right)}{(1+\gamma e^{\eta_1})(1+K)(1+\gamma e^{\eta_2})}\left\{\frac{a_0}{j!}\left(1-\frac{p_0}{p_{2j}}\right)+\sum_{i=1}^{j-1}\frac{b_i}{(j-i)!}\left(\frac{1+\gamma e^{\eta_1}+K(1+\gamma e^{\eta_2})}{\gamma\left(e^{\eta_2}-e^{\eta_1}\right)}+\frac{Ke^{\eta_1}+e^{\eta_2}+\gamma e^{\eta_1}e^{\eta_2}(1+K)}{e^{\eta_2}-e^{\eta_1}}\frac{p_{2i}}{p_{2j}}\right)\right\} \tag{B15}$$

By introducing the following definition for convenience:

$$\lambda_j=-\,b_j\frac{p_{2j}(1+K)\left(1+\gamma e^{\eta_1}\right)\left(1+\gamma e^{\eta_2}\right)}{a_0\,\gamma\left(e^{\eta_2}-e^{\eta_1}\right)p_0};\quad j>0 \tag{B16}$$

with p_z being defined in Eq (30), the expression for the current (23) is finally obtained.

Figure 1. Effect of the chemical kinetics on the NPV-voltammograms (Eqs. (23), (36) and (44)) when the free ion is more lipophilic than the complex ($\Delta\phi^{0'} > 0$)**.** $K = 2,\ \gamma^2 = D_o / D_w = 0.001,\ \tau = 1s,\ z = 1,\ T = 25\ ^{o}\mathrm{C}.\ I_d = zFAc^{*}\sqrt{D_w / \pi\tau}$.

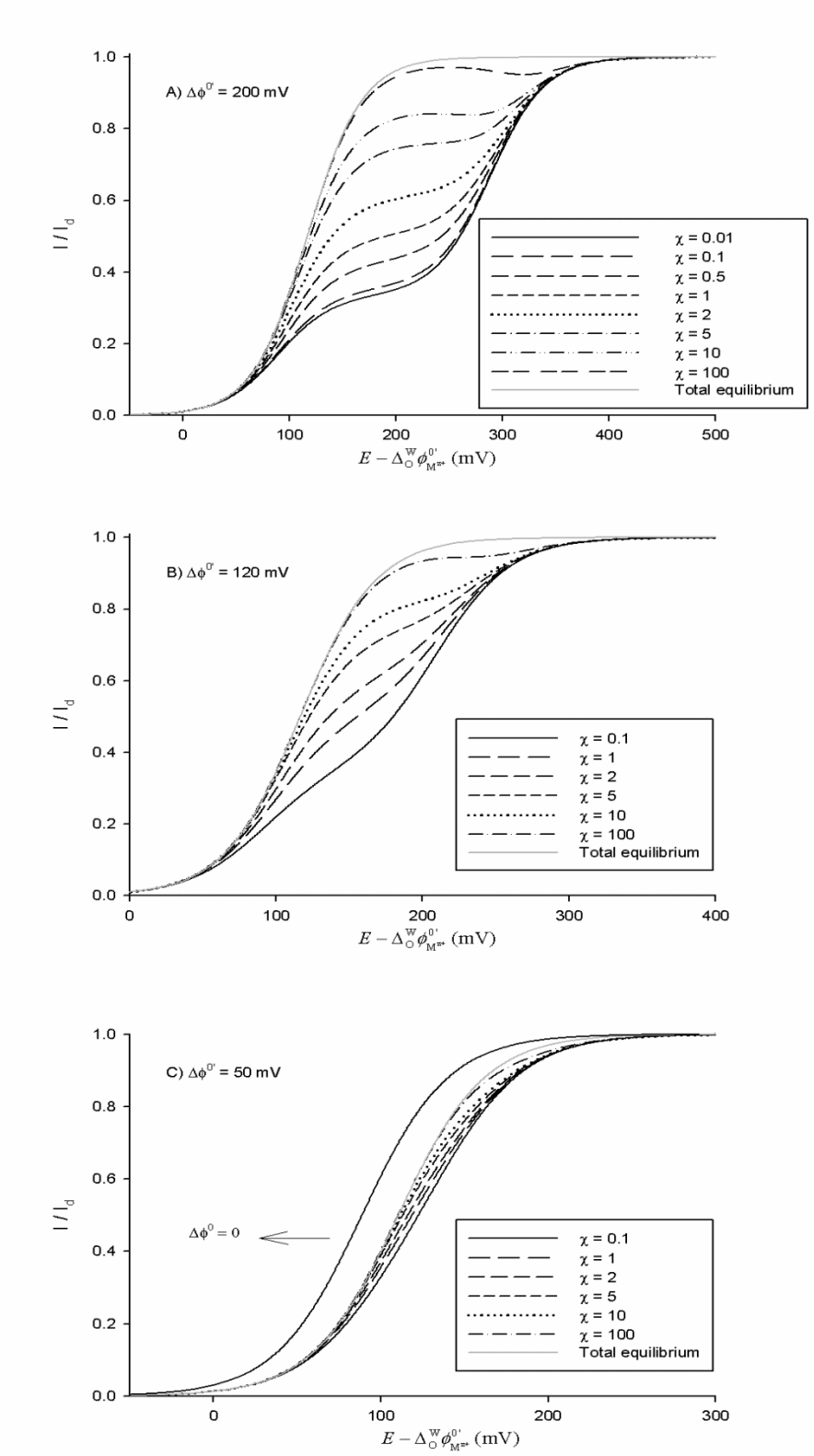

Figure 2. Effect of the chemical kinetics on the NPV-voltammograms (Eqs. (23), (36) and (44)) when the free ion is less lipophilic than the complex ($\Delta\phi^{0'} < 0$)**.** $K = 2,\ \gamma^2 = D_o / D_w = 0.001,\ \tau = 1s,\ z = 1,\ T = 25\ ^{o}\mathrm{C}.\ I_d = zFAc^{*}\sqrt{D_w / \pi\tau}$.

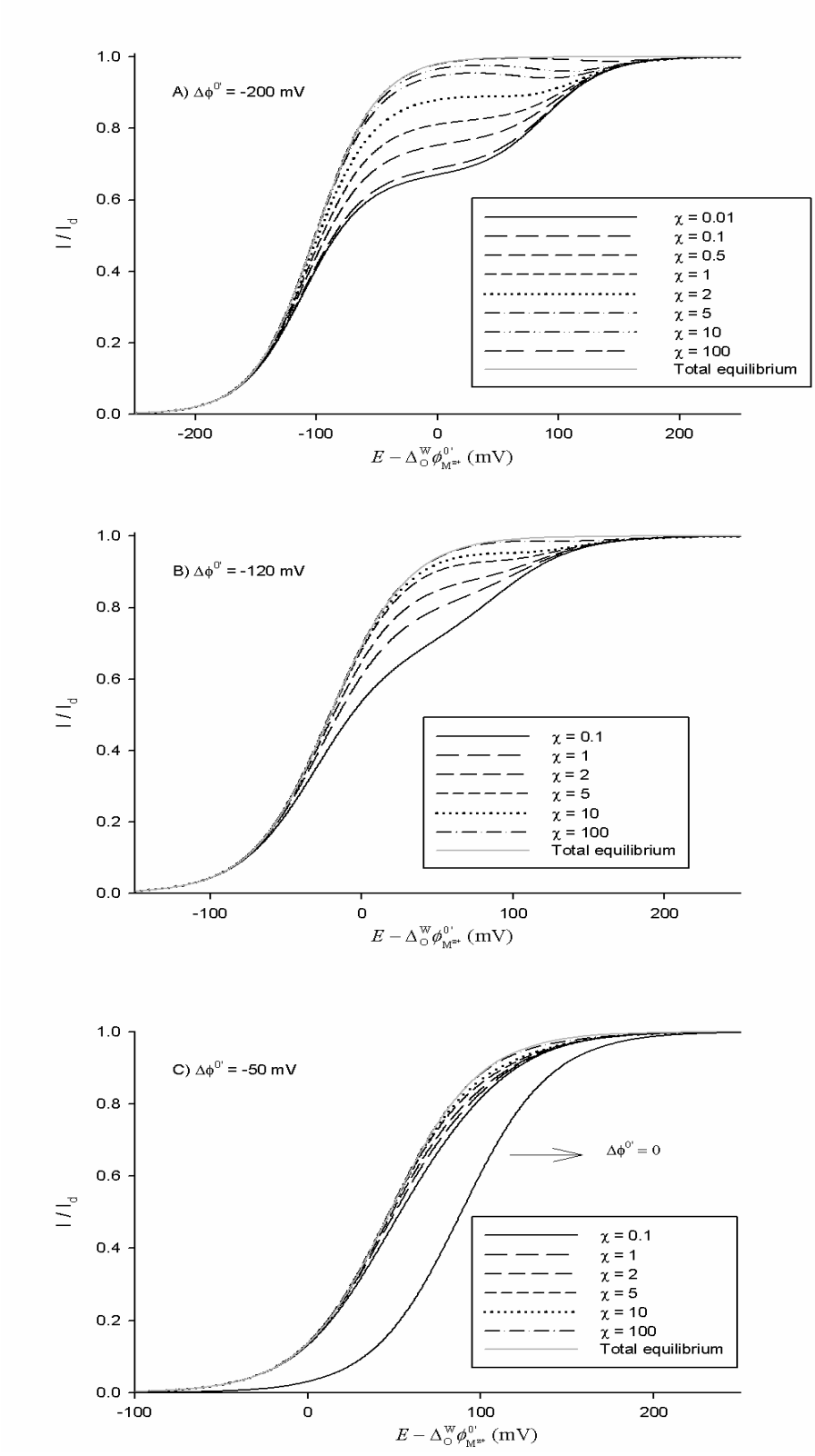

Figure 3. Influence of the equilibrium constant ($K = c^*_{ML} / c^*_M$) on the NPV-voltammograms (Eqs.(23), (36) and (44)) for different chemical kinetics. $\Delta\phi^{0'} = 200\text{mV}$, $\gamma^2 = D_o / D_w = 0.001$, $\tau = 1s$, $z = 1$, $T = 25\,^{\circ}\text{C}$. $I_\text{d} = zFAc^* \sqrt{D_w / \pi\tau}$.

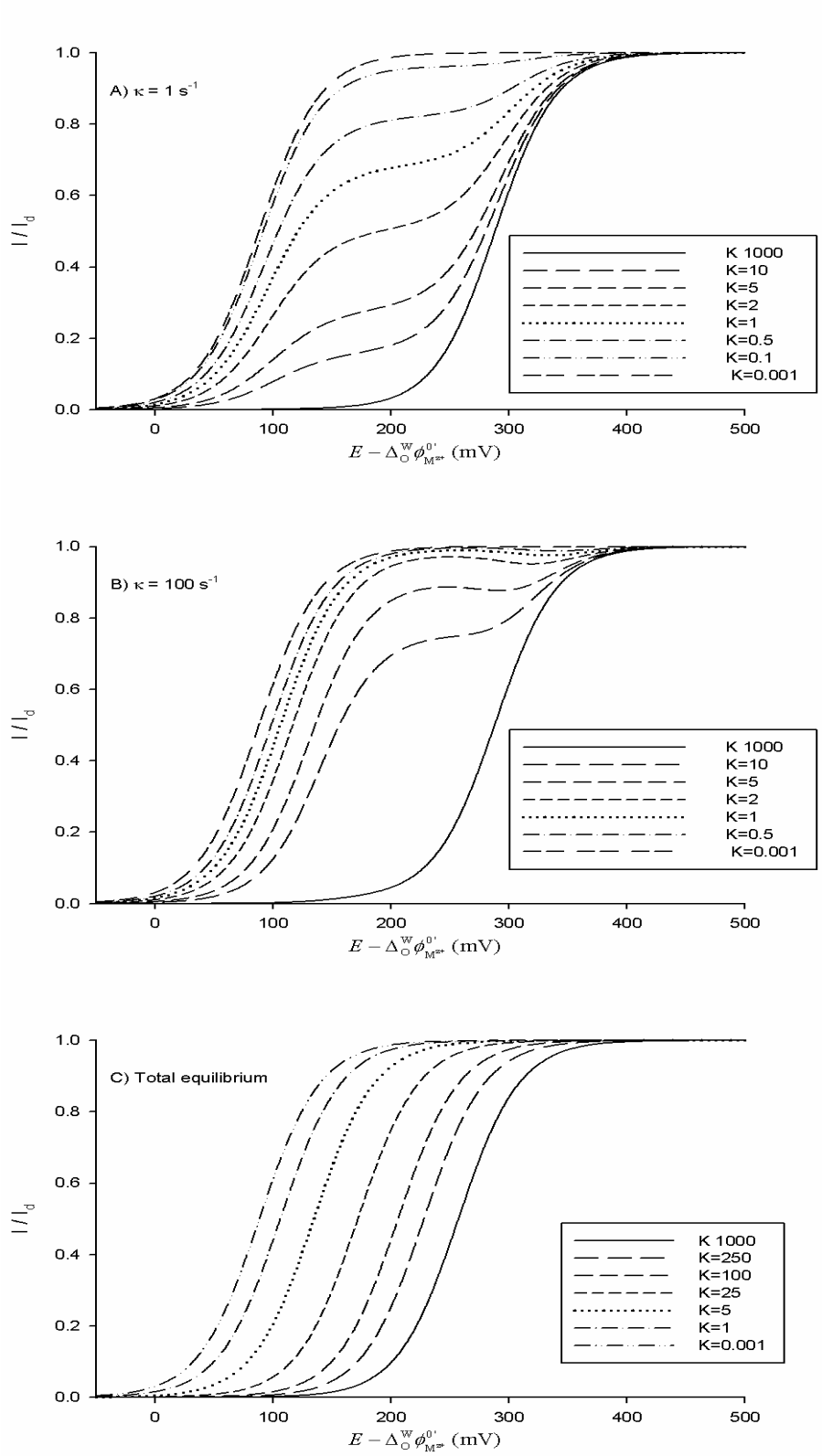

Figure 4. Effect of the ligand concentration (c_L^*) on the NPV-voltammograms (A, Eqs.(23) and (36)), E_{half} (B) and $I_{\lim}^1$ (C) . $\Delta\phi^{0'} = 200\text{mV}$, $\gamma^2 = D_o / D_w = 0.001$, $\tau = 1s$, $z = 1$, $T = 25\,^{\circ}\text{C}$, c^* = 10μM. $K_c = k_1' / k_2 = 10M^{-1}$, $I_{\text{d}} = zFAc^* \sqrt{D_w / \pi\tau}$. $E_{1/2,M^{z+}}$ is given by Eq.(59).

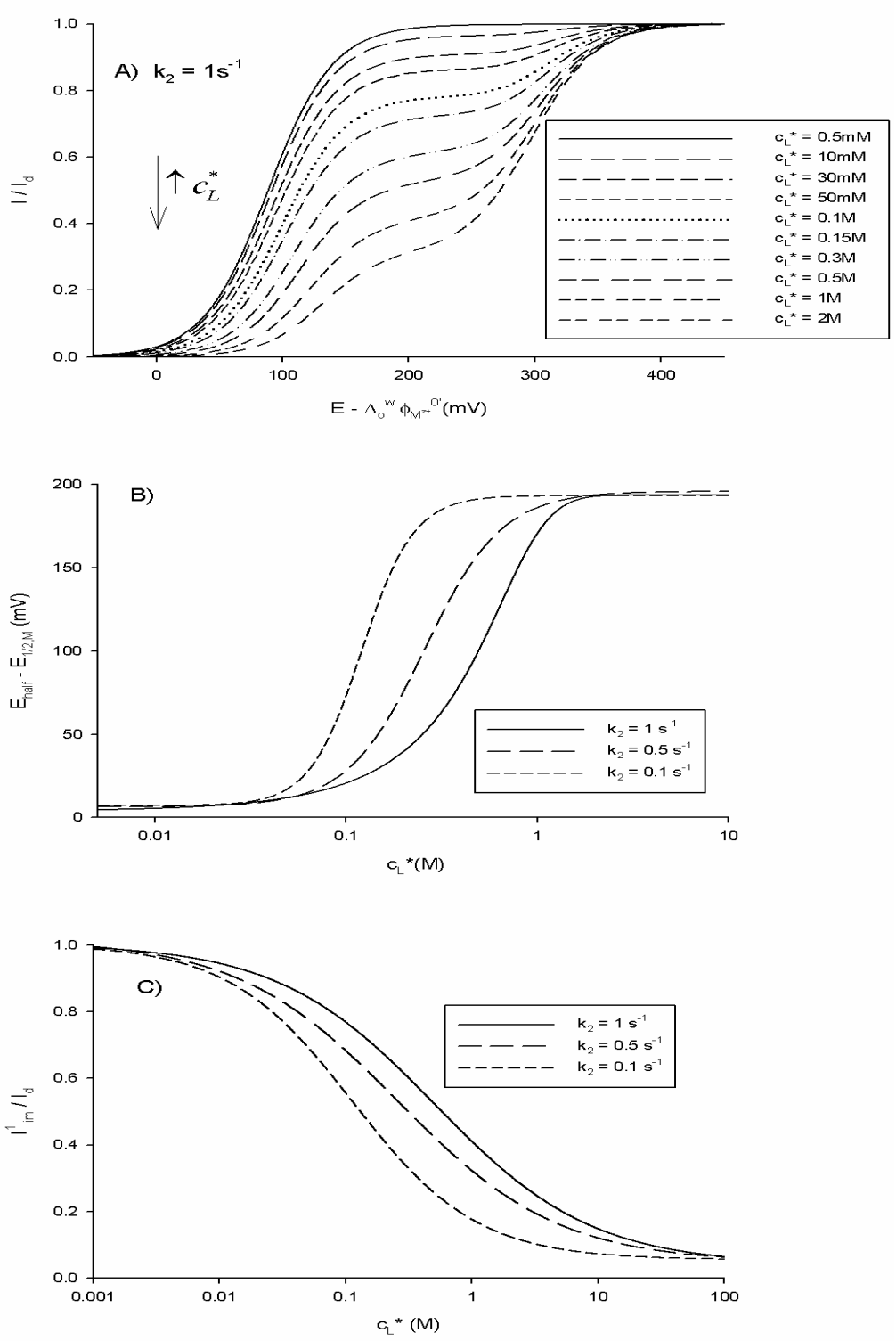

Figure 5. Influence of the chemical kinetics (A) and the equilibrium constant (B) on the dNPV-voltammograms, obtained by differentiation of the corresponding NPV curves (Eqs. (23), (36) and (44)). $\Delta\phi^{0'} = 200\text{mV}$, $\gamma^2 = D_o / D_w = 0.001, \tau = 1s$, $z = 1$, $T = 25\ ^{o}\text{C}$. $I_d = zFAc^* \sqrt{D_w / \pi\tau}$

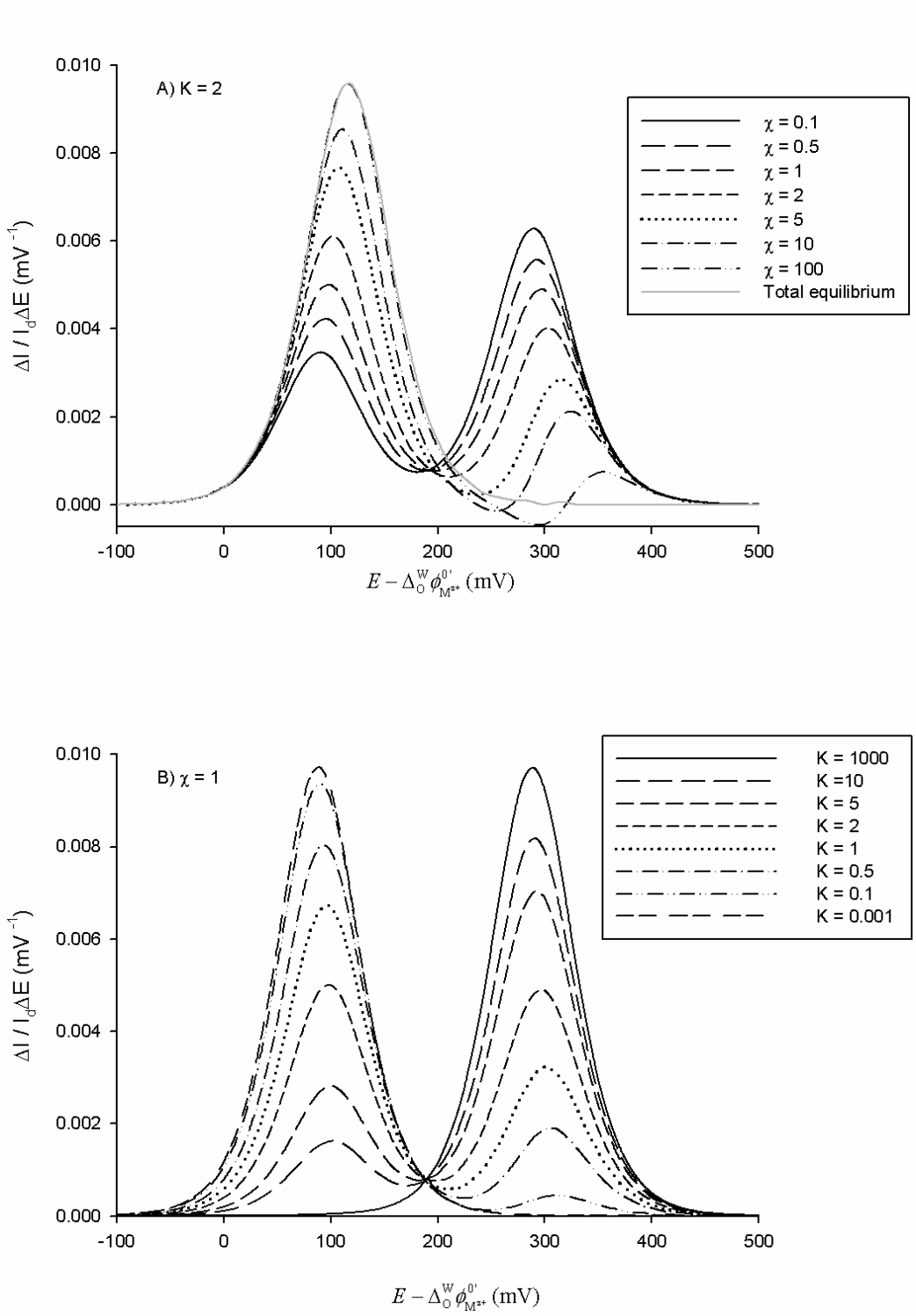

Figure 6. Effect of the chemical kinetics and the equilibrium constant on the chronoamperometric response (Eqs. (23), (36) and (44)). $\Delta\phi^{0'} = 200\text{mV}$, $\gamma^2 = 0.001$, $E - \Delta_{\text{O}}^{\text{W}}\phi_{\text{M}^{z+}}^{0'} = 200\text{ mV}$, $z = 1$, $T = 25\ ^{\text{o}}\text{C}$. $I_{\text{d}} = zFAc^{*}\sqrt{D_w / \pi t}$

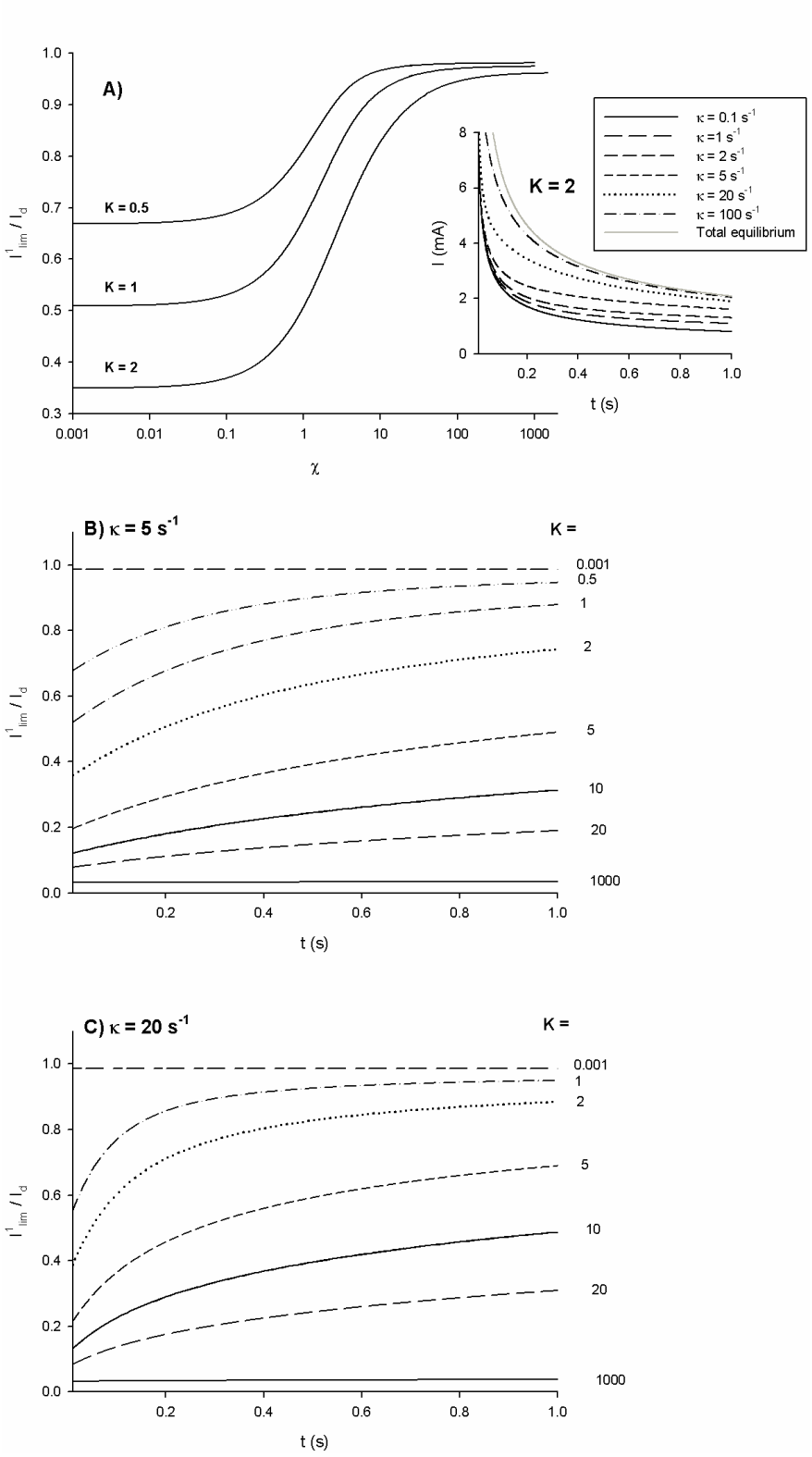

Figure 7. Influence of the scan rate (A), frequency (B) and ligand concentration (C-F) on the CV and SWV curves (Eqs. (52)-(53)), forward peak potential in CV and peak potential in SWV under total equilibrium conditions. A = 12.5 cm^2, $\Delta\phi^{0'} = 200\text{mV}$, $\gamma^2 = D_o / D_w = 0.001$, $z = 1$, $T = 25$ ºC, ΔE = 0.01 mV, E_{sw} = 25 mV, E_s = 2 mV. **A-B:** c^* = 1 mM, K_c = 10 M^{-1}, $c_L^* = 0.2$ M. **C-D:** c^* = 0.1 mM, K_c = 10 M^{-1}, v = 20 mV s^{-1}, f = 10Hz. **E-F:** c^* = 0.1mM, v = 20 mV s^{-1}, f = 10Hz. $E_{1/2,M^{z+}}$ is given by Eq.(59).

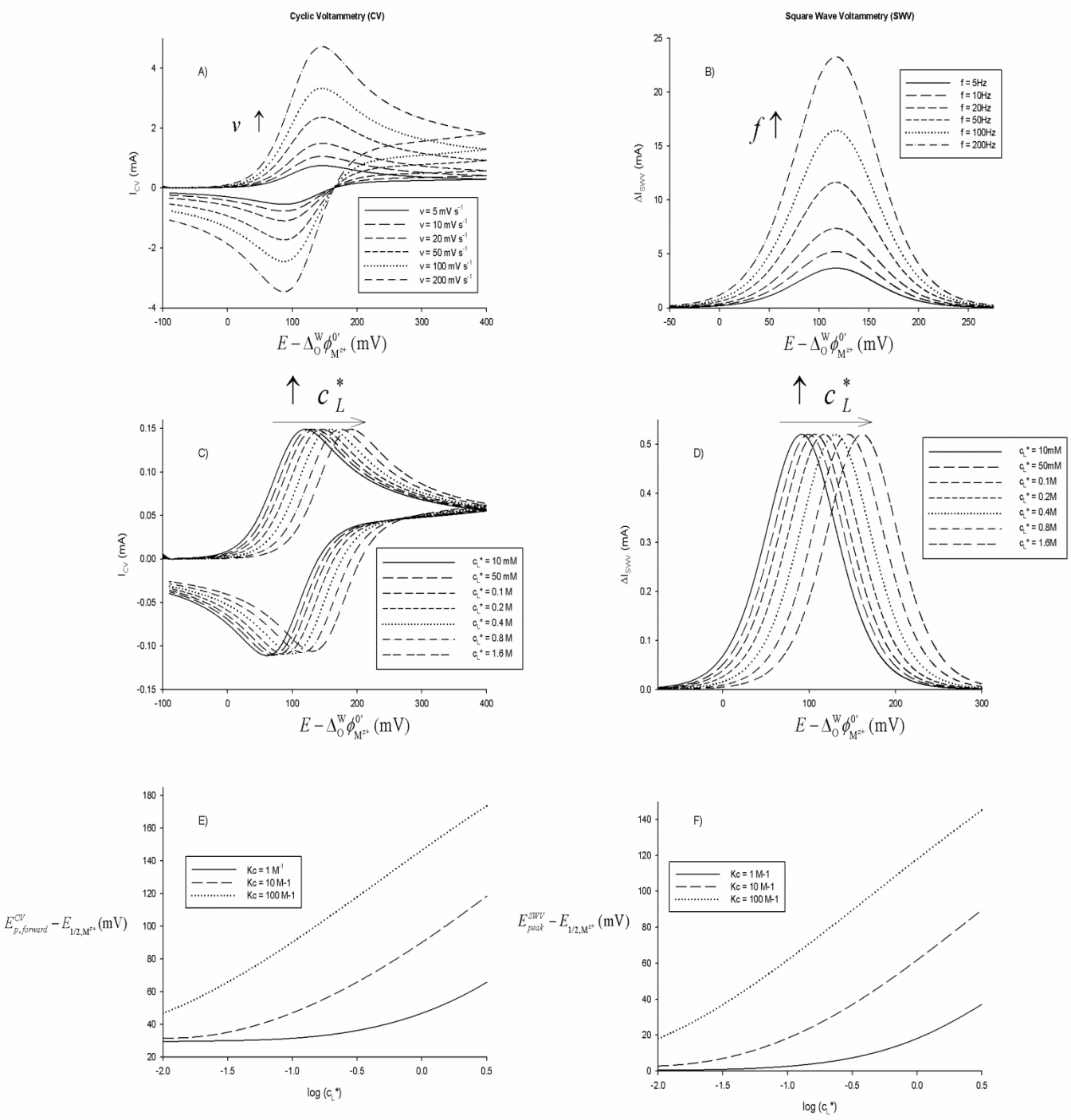

Figure 8. A) Influence of the charge *z* of the ionic species on the forward peak current in CV and **B-C**) the peak current and half-peak width in SWV under total equilibrium conditions. A = 12.5 cm^2, $\Delta\phi^{0'} = 200\text{mV}$, $\gamma^2 = D_o / D_w = 0.001$, $T = 25$ ºC, c^* = 1mM, K = 2, ΔE = 0.01mV, E_s = 2 mV, f = 10Hz.

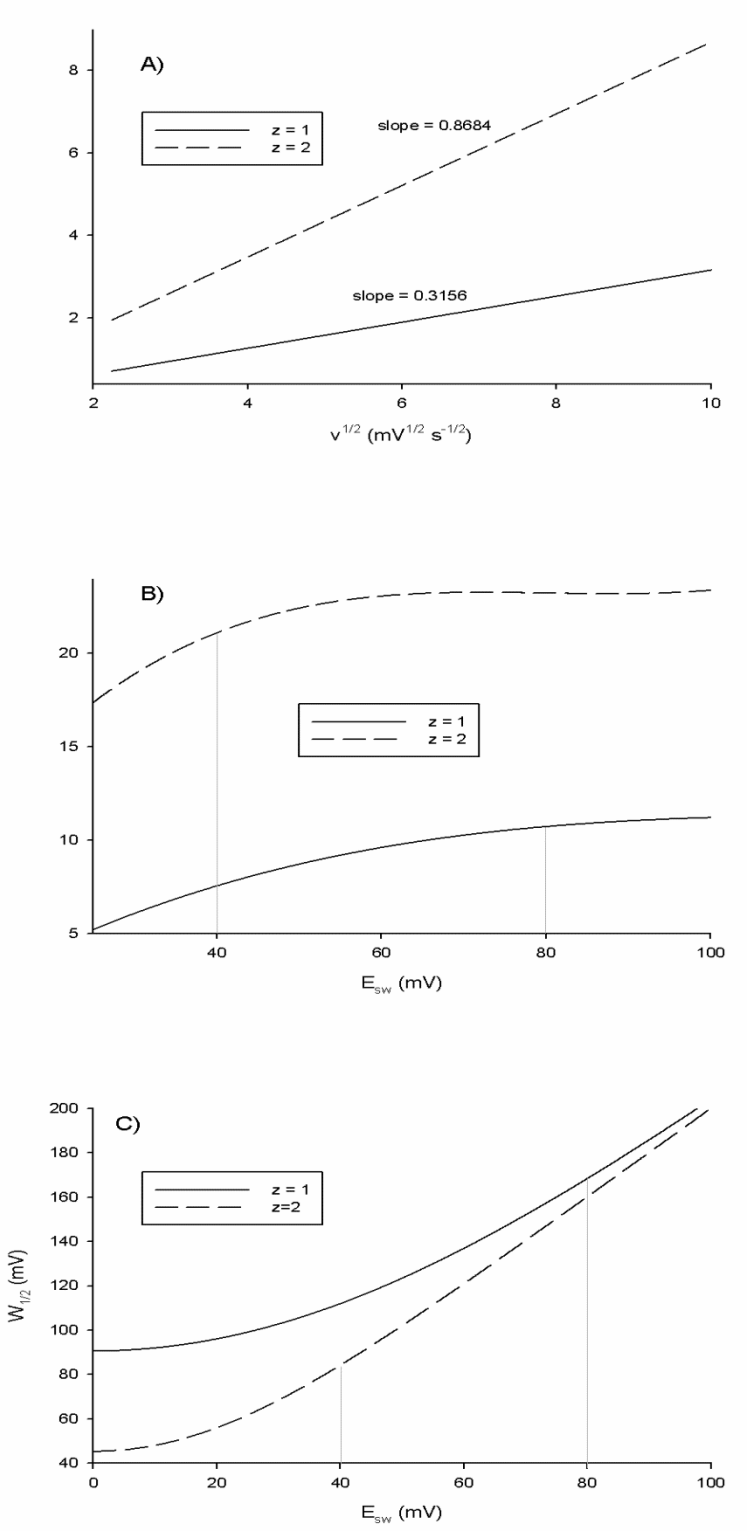

References

1. A. Molina, C. Serna, J. A. Ortuño and E. Torralba, *Annu. Rep. Prog. Chem. Sect. C*, 2012, 108, 126.
2. Z. Samec, *Pure Appl. Chem.*, 2004, 76, 2147.
3. P. Peljo, L. Murtomäki, T. Kallio, H.-J. Xu, M. Meyer, C. P. Gros, J.-M. Barbe, H. H. Girault, K. Laasonen and K. Kontturi, *Journal of the American Chemical Society*, 2012, 134, 5974-5984.
4. V. Beni, M. Ghita and D. W. M. Arrigan, *Biosensors and Bioelectronics*, 2005, 20, 2097.
5. S. Bodor, J. M. Zook, E. Lindner, K. Tóth and R. E. Gyurcsányi, *Analyst*, 2008, 133, 635-642.
6. M. L. Colombo, S. McNeil, N. Iwai, A. Chang and M. Shen, *Journal of The Electrochemical Society*, 2016, 163, H3072-H3076.
7. M. A. Deryabina, S. H. Hansen and H. Jensen, *Analytical chemistry*, 2011, 83, 7388-7393.
8. S. N. Faisal, C. M. Pereira, S. Rho and H. J. Lee, *Physical Chemistry Chemical Physics*, 2010, 12, 15184-15189.
9. G. Herzog, *Analyst*, 2015, 140, 3888-3896.
10. Z. Samec, E. Samcová and H. H. Girault, *Talanta*, 2004, 63, 21.
11. E. Torralba, J. A. Ortuño, A. Molina, C. Serna and F. Karimian, *Anal. Chim. Acta*, 2014, 826, 12.
12. A. J. Bard and L. R. Faulkner, in *Electrochemical Methods, 2nd ed.*, Wiley, New York, 2001.
13. R. G. Compton and C. E. Banks, *Understanding Voltammetry*, World Scientific, 2007.
14. Á. Molina and J. González, Springer, 2015, ch. 3.
15. R. Gulaboski, E. S. Ferreira, C. M. Pereira, M. N. D. S. Cordeiro, A. Garau, V. Lippolis and A. F. Silva, *The Journal of Physical Chemistry C*, 2008, 112, 153-161.
16. P. D. Beattie, R. G. Wellington and H. H. Girault, *J. Electroanal. Chem*, 1995, 396, 317.
17. H. Matsuda, Y. Yamada, K. Kanamori, Y. Kudo and Y. Takeda, *Bull. Chem. Soc. Jpn.*, 1991, 64, 1497.
18. M. A. Deryabina, S. H. Hansen, J. Østergaard and H. Jensen, *The Journal of Physical Chemistry B*, 2009, 113, 7263-7269.
19. R. Ishimatsu, A. Izadyar, B. Kabagambe, Y. Kim, J. Kim and S. Amemiya, *Journal of the American Chemical Society*, 2011, 133, 16300-16308.
20. F. Reymond, V. Chopineaux-Courtois, G. Steyaert, G. Bouchard, P. Carrupt, B. Testa and H. H. Girault, *J. Electroanal. Chem*, 1999, 462, 235.
21. F. Vega Mercado, J. M. Ovejero, R. A. Fernández and S. A. Dassie, *Journal of Electroanalytical Chemistry*, DOI: http://dx.doi.org/10.1016/j.jelechem.2015.08.001.
22. A. Molina, E. Torralba, C. Serna, F. Martínez-Ortiz and E. Laborda, *Phys. Chem. Chem. Phys.*, 2012, 14, 15340.
23. A. Molina, E. Torralba, C. Serna and J. A. Ortuño, *J. Phys. Chem. A*, 2012, 116, 6452.
24. A. Molina, E. Torralba, C. Serna and J. A. Ortuño, *Electrochim. Acta*, 2013, 106, 244.

25. E. Torralba, A. Molina, C. Serna and J. A. Ortuño, *Int. J. Electrochem. Sci.*, 2012, 7, 6771.
26. J. Ortuño, J. Olmos, E. Torralba and A. Molina, *Sensors and Actuators B: Chemical*, 2016, 222, 930-936.
27. H. P. van Leeuwen, R. M. Town, J. Buffle, R. F. Cleven, W. Davison, J. Puy, W. H. van Riemsdijk and L. Sigg, *Environmental science & technology*, 2005, 39, 8545-8556.
28. J. Buffle and M.-L. Tercier-Waeber, *TrAC Trends in Analytical Chemistry*, 2005, 24, 172-191.
29. Y. He, Y. Zheng, M. Ramnaraine and D. C. Locke, *Analytica Chimica Acta*, 2004, 511, 55-61.
30. J. L. Levy, H. Zhang, W. Davison, J. Puy and J. Galceran, *Analytica chimica acta*, 2012, 717, 143-150.
31. Z. Navrátilová and I. Švancara, in *Environmental Analysis by Electrochemical Sensors and Biosensors*, eds. L. M. Moretto and K. Kalcher, Springer New York, 2015, DOI: 10.1007/978-1-4939-1301-5_7, ch. 7, pp. 841-854.
32. P. Chakraborty, A. Manek, S. Niyogi and J. Hudson, *Analytical Letters*, 2014, 47, 1224-1241.
33. A. Molina, F. Martínez-Ortiz, E. Laborda and J. Puy, *Phys. Chem. Chem. Phys.*, 2010, 12, 5396.
34. J. P. Pinheiro, L. S. Rocha, D. Goveia and R. M. Town, *Environmental Chemistry*, 2014, 11, 150-157.
35. L. Sigg, F. Black, J. Buffle, J. Cao, R. Cleven, W. Davison, J. Galceran, P. Gunkel, E. Kalis and D. Kistler, *Environmental science & technology*, 2006, 40, 1934-1941.
36. M. C. Buzzeo, O. V. Klymenko, J. D. Wadhawan, C. Hardacre, K. R. Seddon and R. G. Compton, *The Journal of Physical Chemistry A*, 2003, 107, 8872-8878.
37. R. G. Evans, O. V. Klymenko, P. D. Price, S. G. Davies, C. Hardacre and R. G. Compton, *ChemPhysChem*, 2005, 6, 526-533.
38. D. Zigah, J. Ghilane, C. Lagrost and P. Hapiot, *The Journal of Physical Chemistry B*, 2008, 112, 14952-14958.
39. J. Galvez and A. Molina, *Journal of Electroanalytical Chemistry and Interfacial Electrochemistry*, 1980, 110, 49-68.
40. A. A. M. Brinkman and J. M. Los, *J. Electroanal.Chem*, 1964, 7, 171.
41. J. Koutecký, *Czech. J. Phys.* , 1953, 2, 50.
42. A. Molina, I. Morales and M. López-Tenés, *Electrochem. Commun.*, 2006, 8, 1062.
43. Á. Molina, F. Martínez-Ortiz, E. Laborda and I. Morales, *Journal of Electroanalytical Chemistry*, 2009, 633, 7-14.
44. I. Morales and Á. Molina, *Electrochemistry communications*, 2006, 8, 1453-1460.
45. A. Molina, C. Serna and L. Camacho, *J. Electroanal. Chem*, 1995, 394, 1.
46. M. M. Moreno and A. Molina, *Collect. Czech. Chem. Commun*, 2005, 70, 133.
47. V. Mirčeski, Š. Komorsky-Lovrić and M. Lovrić, *Square-Wave Voltammetry, Theory and Application*, Springer, Heidelberg, 2007.
48. K. Aoki, K. Maeda and J. Osteryoung, *J. Electroanal. Chem*, 1989, 272, 17.
49. A. Molina, J. Gonzalez, E. Laborda and R. G. Compton, *Russian Journal of Electrochemistry*, 2012, 48, 600-609.

50. Á. Molina, E. Laborda, J. M. Gómez-Gil, F. Martínez-Ortiz and R. G. Compton, *Electrochimica Acta*, DOI: http://dx.doi.org/10.1016/j.electacta.2016.01.120.